Dear Editor Remy and referees,

We are very grateful for your time and attentions on this work. Please find below our itemized responses to the referees' comments and a marked-up manuscript. We have addressed all the comments raised by both referees and incorporated them in the revised manuscript.

Thank you for your consideration.

Sincerely,

Sunling Gong, Tianliang Zhao, Lei Zhang et al.

Referee #1

In this manuscript the authors updated the CUACE model with heterogenous reactions and updated dry deposition scheme of particles, and coupled it to the WRF model. This study also evaluated the WRF/CUACE v1.0 model by simulating $PM_{2.5}$, O_3, and NO_2 concentrations in different seasons and different years. This article is clearly written and the methods are generally sound. I recommend the manuscript to be published unless the following comments are addressed:

1. Line 234-235: The authors mentioned "The feedback of chemical species on meteorology in the current WRF/CUACE version is not realized". So in Figure 1, I suggest using dashed line to indicate the influence of chemical variables on WRF module.

Response: Thanks for pointing it out. It has been modified to dashed line in the revised manuscript.

2.Line 290-291: The simulations are relatively poor in the SCB, where the complex terrain poses great challenges to meteorological field simulations. Show the simulations

results of the meteorological fields of the four regions in the supplementary, and compare the simulation results with in-situ observations.

Response: Sincere thanks for the suggestions. The the simulations results of the meteorological fields of the four regions were added in the supplementary (as shown in Table S1). It can be seen that the simulations of meteorological fields in the SCB are relatively poor than the other three regions. For example, the *R*, MB and RMSE values of T2 in the SCB are 0.88, 1.52 ℃ and 2.50 ℃, respectively, while the values in the other three regions vary from 0.91 to 0.93, 0.48 to 1.14 ℃ and 2.01 to 2.39 ℃. The *R* value of WS10 in the SCB is 0.40, which is obviously worse than that of the other three regions (ranging from 0.60 to 0.74), indicating the variation of WS10 in the SCB was not well reproduced by the model. We have added the comparison in Section 5.2.1 in the revised manuscript.

Table S1 Statistical metrics for hourly temperature at 2 m (T2), hourly relative humidity at 2 m (RH2) and hourly wind speed at 10 m (WS10), respectively in the NCP, YRD, PRD and SCB regions.

		Obs	Sim	*R*	MB	ME	RMSE
NCP	T2 (℃)	17.31	18.07	0.91	0.76	1.87	2.34
	RH2 (%)	62.88	51.10	0.80	-11.78	14.47	17.91
	WS10 (m s^{-1})	2.05	2.99	0.64	0.95	1.29	1.60
YRD	T2 (℃)	17.29	17.77	0.93	0.48	1.62	2.01
	RH2 (%)	70.74	64.51	0.82	-6.22	11.28	13.95
	WS10 (m s^{-1})	2.42	3.29	0.74	0.87	1.20	1.47
PRD	T2 (℃)	22.92	24.06	0.91	1.14	2.06	2.39
	RH2 (%)	75.74	67.20	0.78	-8.54	12.73	14.88
	WS10 (m s^{-1})	2.23	3.23	0.60	1.01	1.32	1.61
SCB	T2 (℃)	18.02	19.53	0.88	1.52	2.04	2.50
	RH2 (%)	74.17	59.87	0.73	-14.30	15.98	18.77
	WS10 (m s^{-1})	1.35	2.05	0.40	0.70	0.99	1.24

* All *R* (correlation coefficient) values passed $p < 0.001$.

* Obs and Sim represent the average observations and simulations, respectively.

3. In Section 5.3, the authors evaluated the model performance with and without heterogeneous chemical reactions during a haze event at the Langfang site. How about model improvements at the other sites in the YRD, PRD and SCB region?

Response: Sincere thanks for the suggestions. We have tried our best to collect observations of inorganic secondary aerosols in the three regions. So far, the observations from 3 to 29 December 2013 in Nanjing (located in the YRD) and from 1 to 10 January 2017 in Chengdu (located in the SCB) are obtained for evaluation (Fig. R1). As shown in Fig. R1, simulations of sulfate and nitrate in the two sites are generally improved (change in bias from −95.3 % to -68.4 % in Nanjing and from -88.7 % to -80.1 % in Chengdu for sulfate; change in bias from 83.0 % to 54.6 % in Nanjing and from 67.6 % to 23.5 % in Chengdu for nitrate). The results were added in Section 5.3 in the revised manuscript. We will continue to collect data in the PRD for evaluation in future work.

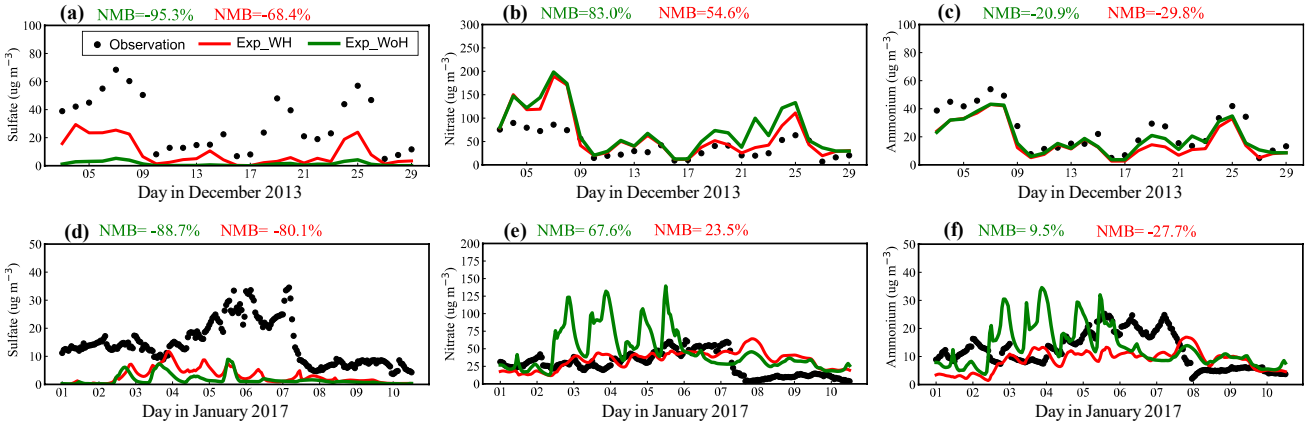

Figure R1. Observed and simulated hourly SIA concentrations from the Exp_WH and Exp_WoH experiments at the (a-c) Nanjing and (d-f) Chengdu site.

4. Line 90-91: This study also updated the dry deposition scheme of particles in CUACE. Please also show the model improvements with and without the updated dry deposition scheme in the supplementary.

Response: Thanks very much for the suggestions. We performed simulations for a winter month (January in 2015) to show the model improvements with and without the updated dry deposition scheme. As shown in Fig. S3, the $PM_{2.5}$ concentrations were commonly underestimated with the Z01 scheme (Fig. R2a), as it tends to overestimate the dry deposition velocity of fine particles (Petroff and Zhang, 2010). The underestimation was improved significantly when the Z01 scheme was

updated to the PZ10 scheme (Fig. R2b). We have added the improvements in the supplementary.

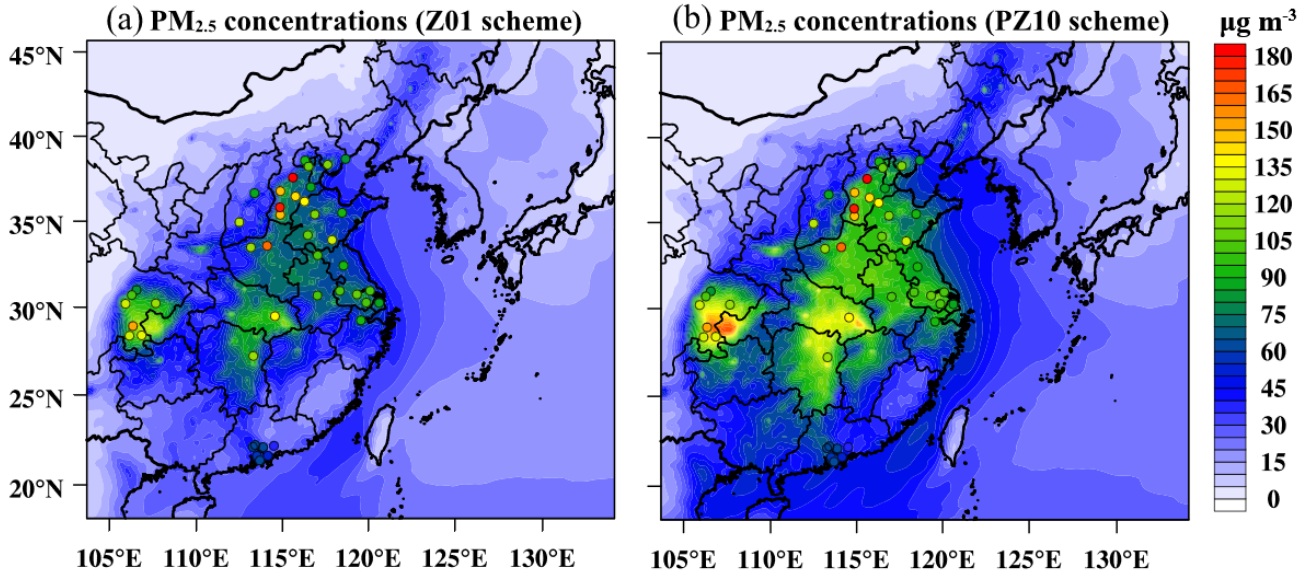

Figure S3. Observed and simulated $PM_{2.5}$ concentrations with (a) Z01 and (b) PZ10 particle dry deposition schemes.

Reference:

Petroff, A. and Zhang, L.: Development and validation of a size-resolved particle dry deposition scheme for application in aerosol transport models, Geoscientific Model Development, 3, 753-769, 2010.

Referee #2

This publication presents a new model called "WRF/CUACE" being the implementation of the chemistry model CUACE into the NWP model WRF version 3. This new model is similar in his implementation to WRF-chem. The authors also presents new developments on aerosol dry deposition scheme and heterogeneous chemistry. The model is evaluated over China on several selected month and deals with $PM_{2.5}$, ozone and NO_2. An other evaluation deals with the model ability to simulate secondary inorganic aerosols and shows the impact of heterogeneous chemistry freshly developed.

This publication is interesting as it presents a new model and proves the feasibility of an easy implementation of a chemistry module into WRF-Chem. But the description of the different compounds is not precise enough and some references are lacking. The available code is very hard to navigate and to understand what part is used, especially concerning the chemical scheme. I just navigate in the directories without trying to compile and run it.

Response: We thank the reviewer for the valuable comments. The description of different compounds is modified to be more precise and the missing references are added. Please see our itemized responses below. To make it easier to navigate the code and to understand what part is used, a schematic showing the flow of information within WRF/CUACE is given in the supplementary (Figure S1).

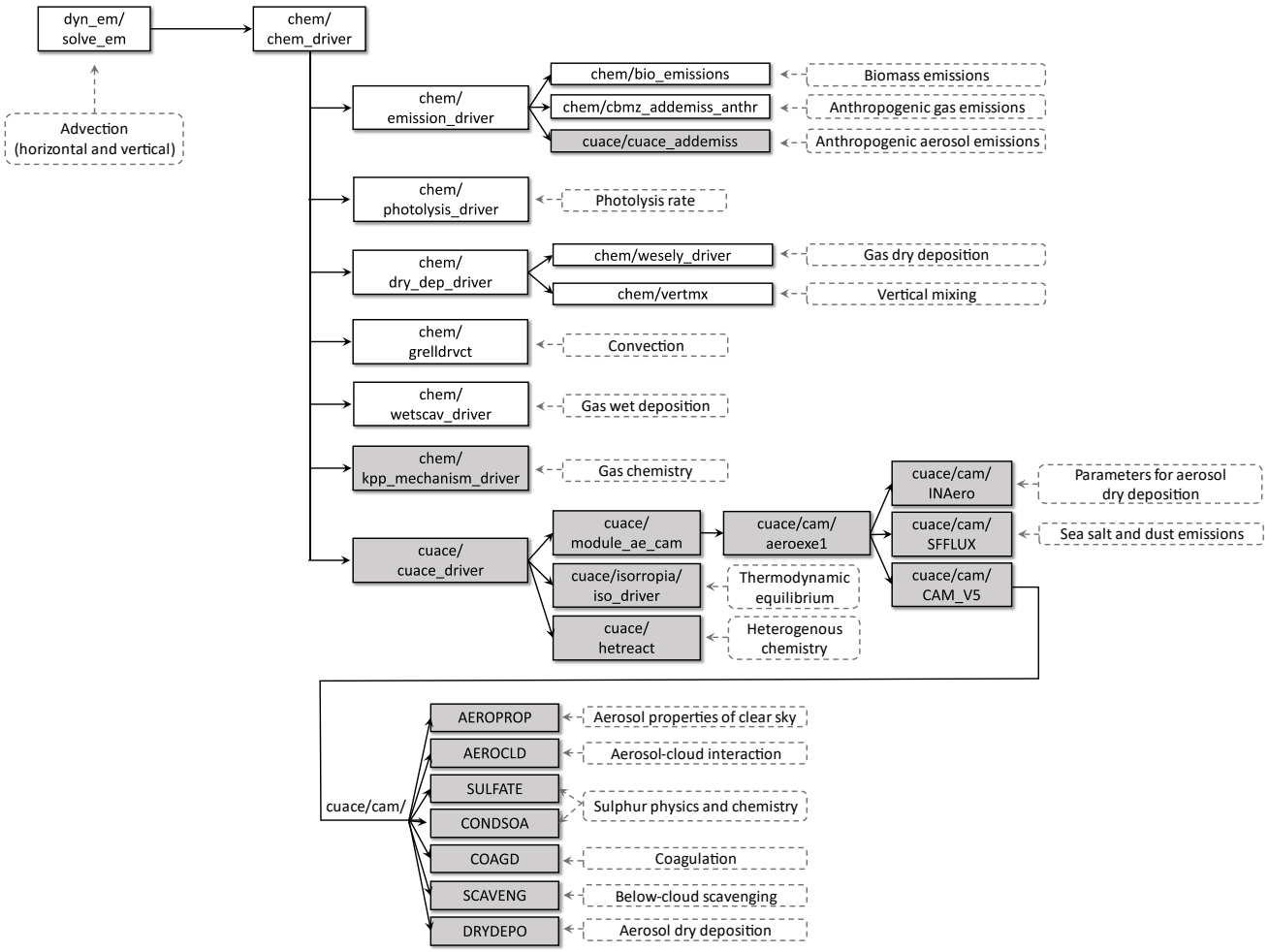

Figure S1. Schematic showing the flow of information within the WRF/CUACE v1.0 model. Gray

boxes indicate the newly added modules to the WRF/Chem framework to build the WRF/CUACE v1.0 model. Dashed boxes are descriptions of each module.

General comments:

This new model aims at replace the actual operational coupled model CUACE with MM5/GRAPES, because the development of the MM5 model has been stopped in favour of WRF. There are no comparison between the actual model and the new WRF/CUACE model. Yet it might have been interesting to compare these two model in order to assess the viability of the newly developed model.

Response: Thanks for this suggestion. We agree with the reviewer on the need to compare the actual model and the new WRF/CUACE model. To this end, we performed a simulation using the MM5/CUACE for a winter month (January 2013), during which a long-lasting haze event occurred in central and eastern China. A new section (Section 5.4) is added in the revised manuscript:

"5.4 Comparison between the MM5/CUACE model and the WRF/CUACE v1.0 model

It is necessary to compare the MM5/CUACE model with the new WRF/CUACE model for the purpose of assessing the viability of the newly developed model. To this end, a simulation was performed using the MM5/CUACE model for a winter month, i.e., January 2013, during which a long-lasting haze event occurred in central and eastern China. The domain setting, anthropogenic emission inventory, initial and boundary fields of meteorology and chemistry are as the same as those of the WRF/CUACE in section 5.1. It should be known that the gas-phase chemistry mechanism and particle dry deposition scheme in MM5/CUACE model is RADM2 and Z01, respectively, that updated to CBM-Z and PZ10 in the new WRF/CUACE model. Physical parameterization used in the

MM5/CUACE is shown in Table S3 in the supplement.

Figure 6 presents a comparison of the modelled and observed daily concentrations of $PM_{2.5}$, O_3, NO_2 and SO_2 in the four regions. It can be seen that the concentrations of $PM_{2.5}$, NO_2 and SO_2 simulated in WRF/CUACE are closer to the observations relative to those of MM5/CUACE model (change in bias from -23.0 % to -19.2 % for $PM_{2.5}$, from 14.7 % to -2.4 % for NO_2 and from -46.2 % to -37.5 % for SO_2). The daily variations of the three species are also relatively better captured by the WRF/CUACE model (reflected by the *R* values changing from 0.45 to 0.62 for $PM_{2.5}$, from 0.41 to 0.49 for NO_2 and from 0.19 to 0.32 for SO_2). For O_3, the differences of statistical metrics between the two models are not obvious. The MM5/CUACE model performed with a slightly smaller bias of -10.7 % but with a lower R value of 0.50, which are 14.3 % and 0.55, respectively in the WRF/CUACE simulation. In summary, the new WRF/CUACE model performed better than the MM5/CUACE model in simulating air pollutants."

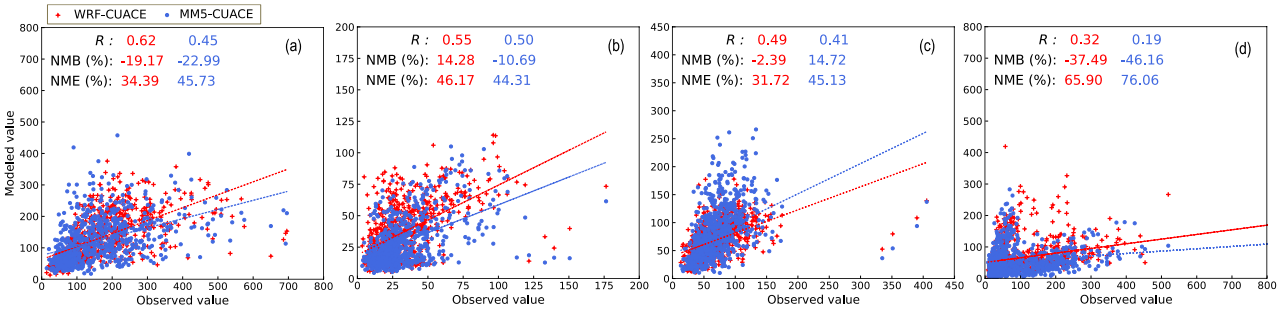

Figure 6. Scatter plots of simulated, with (blue) MM5/CUACE and (red) WRF/CUACE, and observed daily concentrations of (a) $PM_{2.5}$, (b) O_3, (c) NO_2 and (d) SO_2.

It is not very clear how the different processes are treated by the different sub-model. For example at page 4 on line 108: "emissions, gaseous chemistry, and a size-segregated multicomponent aerosol algorithm (Zhou et al., 2012), and has been designed as a unified chemistry module". But on line 130 the authors said CUACE also treat particle dry deposition. The authors need to clarify what processes is done by

which model. This includes the Figure 1 where it would be interesting to have a CUACE box that shows what in included in CUACE. Also on Figure 1 processes done by WRF need to be in the WRF box (convection for example). Also consider to rewrite the section 4, as a reader does not necessarily know how the model WRF-Chem works.

Response: Sincere thanks for pointing this out. The CUACE is a unified chemistry module, in which most of the physical and chemical processes are treated (Fig. 1), except advection and convection processes that done by its host model. In the manuscript, the sentence "*The CUACE module is a unified atmospheric chemistry module incorporating three major functional modules: emissions, gaseous chemistry, and a size-segregated multicomponent aerosol algorithm (Zhou et al., 2012), and has been designed as a unified chemistry module*" has been revised as "The CUACE is a unified chemistry module, which treats most of the physical and chemical processes, except advection and convection processes that done by its host model. The main processes treated in CUACE module include emissions, gas chemistry, dry and wet deposition, vertical mixing, aerosol-cloud interaction, and clear-air (i.e., aerosol produced by chemical transformation of their precursors together with particle nucleation, condensation and coagulation) (An et al., 2016; Zhou et al., 2012; Gong et al., 2003).".

We have revised the Figure 1 and added Figure S1 to clearly describe the different processes treated in the different sub-model following your suggestion, and state in Section 4: "The flow of the major process splitting in the coupled WRF/CUACE v1.0 model is illustrated in Fig. 1 with the structure of related subroutines given in Fig. S1 in the supplement. The WRF/CUACE v1.0 model uses several modules of the original WRF/Chem model, i.e., modules of advection, vertical mixing, convection, biomass emissions, anthropogenic gas emissions, photolysis and gas dry/wet deposition (Fig. S1). As described in Section 2.2, the CBM-Z mechanism is newly added with the KPP protocol (Damian et al., 2002) to replace the RADM2 mechanism in the original CUACE module. An interface procedure, cuace_driver,

is designed to integrate the core sections of the aerosol physical and chemical processes of the CUACE module with the WRF framework (Fig. S1).”

We have carefully revised the Section 4 for readers to more easily understand how the WRF-Chem model works. For example, we added more description of WRF-Chem: “WRF-Chem is a meteorology-chemistry coupled model. In the chemical module of the WRF-Chem, the processes are split to emissions, vertical mixing, dry deposition, convection, gas chemistry, cloud chemistry, aerosol chemistry and wet deposition, all of which are integrated in an interface procedure (chem_driver). Advection process is treated in the WRF model. Information, such as rainfall rates, vertical mixing coefficients and convective updraft properties, is provided by WRF to calculate the processes treated in the chemical module. WRF-Chem uses registry tools for automatic generation of application code. Physical and chemical variables, as well as options of parameterization schemes are coded in files (such as registry.chem) in the directory of WRFV3/Registry, which provides the convenience for developers to add variables and options.”.

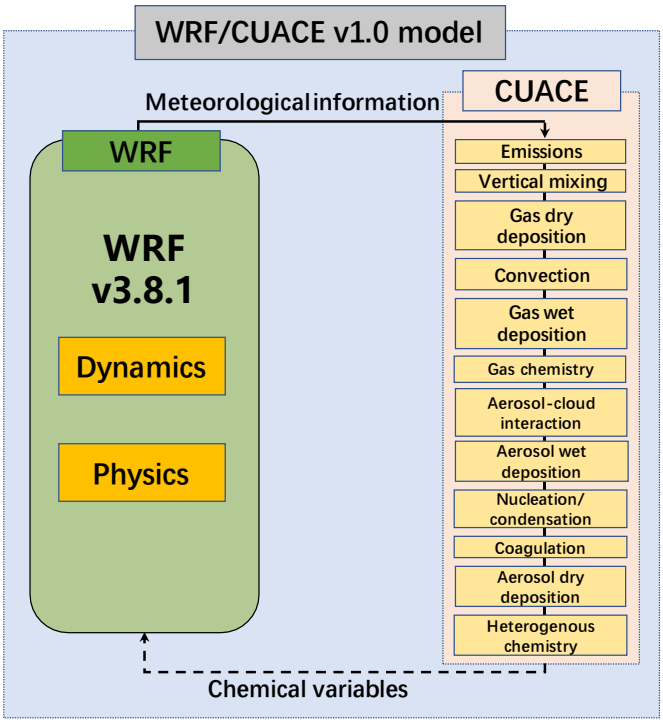

Figure 1. Schematic of modules in the WRF/CUACE v1.0 system.

In section 3.2, the authors describe the added heterogeneous chemistry added to the model. I wonder if "Aerosol" stands for all the aerosols in the model, treated the same way or if only a sample of all aerosols are considered in the reaction. Also, the way the reactions are written may let think that the aerosol used as a reactant disappear, or I guess it only acts as a support for the reaction.

Response: Sorry for the unclear descriptions. The "Aerosol" stands for all the aerosols in the model. Aerosol in the reactions only acts as a support. We state in the revised Section 3.2 ""<u>Aerosol" in the reactions stands for all the aerosols in the model"</u>, and rewrite the forms of heterogeneous chemical reactions from "… + Aerosol → …" to "… $\xrightarrow{\text{Aerosol}}$ **…".**

The description of the model CUACE is not precise enough, essentially concerning the chemical scheme and the reference Zhou et al, (2012) does not either. You claim that RADM2 has 121 reactions, but there are more in Stockwell et al, (1990). Please add the reference for RADM2 and explain the differences between the original publication and your version of RADM2. In section 4, authors explain they added the possibility to use the chemical scheme CBM-Z using KPP. But they do not precise which chemical scheme is finally used. If it is RADM2, then this section should be in the conclusion as future work. If it is CBM-Z then it should be on section 2.2 about CUACE module and more developed: number of species, number of reactions, number of photochemical reactions, way the photochemical reactions are taken into account (especially above the 100hPa upper limit), etc.

Response: Thanks very much for pointing out it. We have confirmed with Zhou and checked the code of CUACE. There are totally 136 chemical reactions and 21 photochemical reactions in the RADM2 scheme in CUACE model. We have corrected the mistake in the revised Section 2.2.

Sorry for the unclear description of which chemical scheme is finally used. The

RADM2 mechanism in the original CUACE module is discarded in the WRF/CUACE v1.0 model, so the CBM-Z mechanism is finally used for simulation. We state in the Section 2.2: "As the gaseous chemistry (RADM2) in the CUACE module is not computationally economic and it is hard coded, which means that it is not conducive to adapting chemical reactions in the future, the CBM-Z photochemical mechanism (Zaveri and Peters, 1999) with a better computational efficiency is added with the KPP protocol (Damian et al., 2002) to replace the RADM2 mechanism.".

Following your suggestion, we have revised the section 2.2 to detail the chemical scheme CBM-Z: "CBM-Z mechanism (Zaveri and Peters, 1999) contains 55 species, 114 reactions and 20 photochemical reactions. It is based on the widely used Carbon Bond Mechanism (CBM-IV) and uses the lumped structure approach for condensing organic species and reactions. CBM-Z extends the CBM-IV to include revised inorganic chemistry, explicit treatment of the lesser reactive paraffins, methane and ethane, revised treatments of reactive paraffin, olefin, and aromatic reactions, inclusion of alkyl and acyl peroxy radical interactions and their reactions with NO_3, inclusion of organic nitrates and hydroperoxides, and revised isoprene chemistry. Currently, stratospheric chemistry is not included in the CUACE module. Species (i.e, CH_4, CO, O_3, NO, NO_2, HNO_3, N_2O_5 and N_2O) above a specified pressure level are fixed to climatological values. Between the specified pressure level and the tropopause level, the species was relaxed with a 10-day relaxation factor."

The present paper deals with a new combination of a NWP and a chemistry model. But only a part of the chemistry is evaluated. It would have been interesting to evaluate the meteorological fields during the simulation made. Moreover the fact that the SCB region seems badly represented for $PM_{2.5}$ is due to the complex terrain could be illustrated.

Response: Sincere thanks for the suggestions. The simulated temperature at 2 m

(T2), relative humidity at 2 m (RH2) and wind speed at 10 m (WS10) were selected for evaluation. Table S1 shows the observation mean, simulation mean, correlation coefficient (*R*), MB, ME and RMSE of the meteorological fields in the NCP, YRD, PRD and SCB, respectively.

The MB and RMSE for T2 vary from 0.48 to 1.14 ℃ and from 2.01 to 2.50 ℃, respectively, indicating surface temperatures are slightly overestimated in the four regions. The *R* value for T2, ranging from 0.88 to 0.93, indicates the variation trends are well captured by the model. The model underestimates RH2 in the four regions with the MB ranging from -6.22 to -14.30 % and the RMSE ranging from 13.95 to 18.77 %, which are comparable with previous studies in China (Wang et al., 2014; Gao et al., 2016). The RMSE for WS10 in the four regions vary from 1.47 to 1.61 m s^{-1}, fall within the "good" model performance criteria (little than 2 m s^{-1}) proposed by Emery et al. (2001). However, it should be noted that the *R* for WS10 in the SCB is relatively poor, indicating the variation trends were not well captured. Generally, the model performed best in the YRD, followed by the PRD and NCP, and performed worst in the SCB for meteorological fields. We have added the evaluation in Section 5.2.1 in the revised manuscript.

Table S1 Statistical metrics for hourly temperature at 2 m (T2), hourly relative humidity at 2 m (RH2) and hourly wind speed at 10 m (WS10), respectively in the NCP, YRD, PRD and SCB regions.

		Obs	Sim	*R*	MB	ME	RMSE
NCP	T2 (℃)	17.31	18.07	0.91	0.76	1.87	2.34
	RH2 (%)	62.88	51.10	0.80	-11.78	14.47	17.91
	WS10 (m s^{-1})	2.05	2.99	0.64	0.95	1.29	1.60
YRD	T2 (℃)	17.29	17.77	0.93	0.48	1.62	2.01
	RH2 (%)	70.74	64.51	0.82	-6.22	11.28	13.95
	WS10 (m s^{-1})	2.42	3.29	0.74	0.87	1.20	1.47
PRD	T2 (℃)	22.92	24.06	0.91	1.14	2.06	2.39
	RH2 (%)	75.74	67.20	0.78	-8.54	12.73	14.88
	WS10 (m s^{-1})	2.23	3.23	0.60	1.01	1.32	1.61
SCB	T2 (℃)	18.02	19.53	0.88	1.52	2.04	2.50
	RH2 (%)	74.17	59.87	0.73	-14.30	15.98	18.77
	WS10 (m s^{-1})	1.35	2.05	0.40	0.70	0.99	1.24

* All R (correlation coefficient) values passed $p < 0.001$.

* Obs and Sim represent the average observations and simulations, respectively.

Reference:

Wang, Y., Zhang, Q., Jiang, J., Zhou, W., Wang, B., He, K., Duan, F., Zhang, Q., Philip, S., and Xie, Y.: Enhanced sulfate formation during China's severe winter haze episode in January 2013 missing from current models, J. Geophys. Res.-Atmos., 119, 10425–10440, doi:10.1002/2013JD021426, 2014.

Gao, M., Carmichael, G. R., Wang, Y., Ji, D., Liu, Z., and Wang, Z.: Improving simulations of sulfate aerosols during winter haze over Northern China: the impacts of heterogeneous oxidation by NO2, Frontiers of Environmental Science & Engineering, 10, 2016.

Emery, C., Tai, E., and Yarwood, G.: Enhanced meteorological modeling and performance evaluation for two Texas ozone episodes, in: Prepared for the Texas Natural Resource Conservation Commission, ENVIRON International Corporation, Novato, CA, USA, 2001.

In section 5.2, the authors talk about the negative bias in winter in NCP region by saying that the model misses secondary aerosols. But in summer it seems to be a positive bias almost as dramatic as the negative bias in winter. Do the authors have an explanation for this bias?

Response: Thanks for pointing out it. According to our analysis, the positive bias in summer in NCP is mainly due to the uncertainty in anthropogenic emissions. It is known that $PM_{2.5}$ concentration is mainly driven by primary emissions, meteorology and chemical reactions. Table S2 shows the statistical metrics for hourly meteorological fields in winter and summer in the NCP. It can be seen that bias of summer meteorological fields is reasonable, and is comparable to those in winter (Table S2) as well as to those in the YRD and PRD (Table S1), which indicate bias in meteorological fields is not the reason. Additionally, In the YRD and PRD, where the uncertainties of anthropogenic emissions are generally known as less than that of NCP, the bias of $PM_{2.5}$ between winter and summer are comparable (Table 3), implying chemical formation of $PM_{2.5}$ in summer is not overestimated by the WRF/CUACE v1.0 model. Therefore, it could be inferred that uncertainties in

the emission inventory in the NCP lead to the dramatic positive bias of $PM_{2.5}$. We have added the analysis in Section 5.2.2 in the revised manuscript.

Table S2 Statistical metrics for hourly temperature at 2 m (T2), hourly relative humidity at 2 m (RH2) and hourly wind speed at 10 m (WS10), respectively in winter and summer in the NCP.

NCP region		Obs	Sim	*R*	MB	ME	RMSE
Winter	T2 (℃)	1.59	2.01	0.85	0.42	1.67	2.14
	RH2 (%)	62.65	53.17	0.75	-9.48	14.18	18.18
	WS10 (m s^{-1})	1.82	2.64	0.62	0.82	1.15	1.46
Summer	T2 (℃)	27.48	28.88	0.89	1.40	1.89	2.38
	RH2 (%)	72.79	59.61	0.84	-13.18	13.98	16.42
	WS10 (m s-1)	1.93	2.42	0.54	0.49	1.00	1.27

Table 3 Statistical metrics for hourly $PM_{2.5}$ in four haze contaminated areas (2013–2017), in which bold, normal , and italic font for MFB and MFE correspond to the "excellent", "good", and "average" levels in Morris et al. (2005), respectively.

	R	MB	ME	NMB	NME	MFB	MFE
		μg m^{-3}	μg m^{-3}	%	%	%	%
NCP	0.59	-5.0	44.5	-5.4	47.5	3.3	49.1
Winter	0.59	-45.0	67.7	-28.4	42.7	-22.5	47.0
Spring	0.57	-9.5	28.0	-14.0	41.1	-20.7	47.4
Summer	0.47	33.9	42.9	55.1	69.8	*44.9*	*56.3*
Autumn	0.63	-0.8	39.2	-0.9	45.4	9.0	45.9
YRD	0.71	12.9	26.9	21.8	45.3	21.1	42.9
Winter	0.75	6.0	30.6	6.4	32.5	**8.5**	**34.1**
Spring	0.49	14.2	26.3	25.4	47.1	19.1	40.0
Summer	0.56	16.4	23.3	47.8	67.9	26.7	49.4
Autumn	0.66	15.1	27.3	28.7	51.8	29.5	48.0
PRD	0.68	5.3	17.1	13.1	42.1	8.6	40.1
Winter	0.56	3.0	20.5	5.0	34.6	**5.5**	**34.4**
Spring	0.64	6.9	17.6	19.5	49.7	4.2	45.6
Summer	0.68	2.8	8.5	14.8	44.4	5.9	39.0
Autumn	0.54	8.6	21.8	17.7	45.2	18.3	41.9
SCB	0.59	7.6	31.3	12.2	50.3	*20.7*	*51.4*
Winter	0.41	-13.3	46.7	-11.5	40.4	-8.3	45.2
Spring	0.49	4.1	22.4	8.4	45.9	11.4	46.1
Summer	0.40	21.6	28.2	60.4	78.6	*38.7*	*58.9*
Autumn	0.58	15.9	28.2	31.4	55.7	*37.2*	*54.3*

The authors detailed the implementation of the new dry deposition scheme. Also in the conclusion, they wrote "it is difficult to evaluate the dry deposition process is improved", but they did not present any comparison between the two parametrization. A comparison over the already used observed concentrations for the evaluation might be a start for evaluating the improvement.

Response: Sincere thanks for the suggestions. We have added the comparison between the two parametrization in the revised Section 3.1 "<u>The most significant difference between the Z01 and PZ10 scheme is the treatment of *Rs*, which stands for the dry velocity contributed by surface resistance, including the effect of Brownian diffusion, turbulent impaction, interception and rebound. According to the study of Wu et al., (2018), dry deposition velocity of fine particles is strongly affected by the Brownian diffusion and turbulent impaction. Thereby, it could be inferred that the Z01 scheme is prone to overestimate the effect of Brownian diffusion and turbulent impaction. In a recent study by Emerson et al. (2020), with observationally constrained approach, the Z01 scheme was revised to be with weaker effect of Brownian diffusion, and as a result, got better performance in simulating the dry deposition velocity of fine particles.</u>".

Following the suggestions, we performed simulations for a winter month (January 2015) to show the model improvements with and without the updated dry deposition scheme. As shown in Fig. S3, the $PM_{2.5}$ concentrations were commonly underestimated with the Z01 scheme (Fig. S3a), as it tends to overestimate the dry deposition velocity of fine particles (Petroff and Zhang, 2010). The underestimation was improved significantly when the Z01 scheme was updated to the PZ10 scheme (Fig. S3b). We have added the comparison in the supplementary, and state in the conclusions: "<u>With the observed $PM_{2.5}$ concentrations, model improvements with and without the updated dry deposition scheme are preliminary evaluated (as shown in Figure S3 in the supplement).</u>".

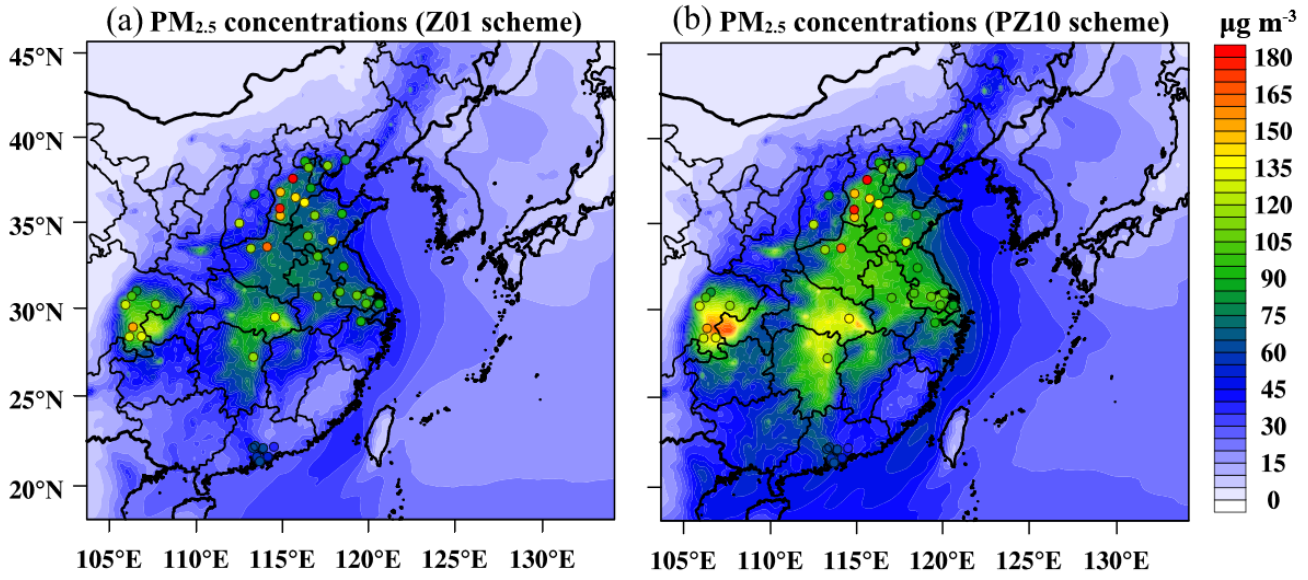

Figure S3. Observed and simulated $PM_{2.5}$ concentrations with (a) Z01 and (b) PZ10 particle dry deposition schemes.

Reference:

Petroff, A. and Zhang, L.: Development and validation of a size-resolved particle dry deposition scheme for application in aerosol transport models, Geoscientific Model Development, 3, 753-769, 2010.

Emerson, E. W., Hodshire, A. L., DeBolt, H. M., Bilsback, K. R., Pierce, J. R., McMeeking, G. R., and Farmer, D. K.: Revisiting particle dry deposition and its role in radiative effect estimates, Proceedings of the National Academy of Sciences, doi: 10.1073/pnas.2014761117, 2020. 202014761, 2020.

Specific comments:

Page 3, line 70: A or several reference for WRF are missing here.

Response: Thanks for pointing out it. We have added the reference (Skamarock, 2008) in the revised manuscript.

Reference:

Skamarock, W. C., Klemp, J. B., Dudhia, J., Gill, D. O., Barker, D. M., Duda, M. G., Huang, X.-Y.,

Wang, W., and Powers, J. G.: A description of the Advanced Research WRF version 3, National Center for Atmospheric Research Tech. Note, NCAR/TN-475+STR, 113 pp., 2008.

Page 4, line 114: Please add 'primary' for organic carbon if it is the case. Otherwise add a sentence to explain how secondary organic aerosols are treated.

Response: The 'primary' was added.

Page 4, line 123: Please add the fact that Xi is the mixing ratio of the species i.

Response: It has been added.

Page 4, line 124: I do not understand what the authors mean by clear-air tendency, please explain.

Response: Thanks for pointing out it. The clear-air tendency means aerosol mass produced by chemical transformation of their precursors together with particle nucleation, condensation and coagulation form the clear-air processes (Gong et al., 2003). We have added the explanation in the first paragraph in Section 2.2.

Reference:

Gong, S. L., Barrie, L. A., J.-P. Blanchet, Salzen, K. v., U. Lohmann, and Lesins, G.: Canadian Aerosol Module: A size-segregated simulation of atmospheric aerosol processes for climate and air quality models 1. Module development, Journal of Geophysical Research, 108, 2003.

*Page 5/6: Generally speaking this part on deposition is not always easy to read because there are parenthesis missing for function [e.g. tanhη → tan(hη)] or multiply sign also missing (e.g. LAIETh → LAI*ET*h).*

Response: Thanks for pointing out it. We have carefully checked page 5/6. The parenthesis and multiply sign missed in this part has been added.

Page 5, line 132: "that developed by Petroff and Zhang" → "~~that~~ developed by Petroff and Zhang" for example.

Response: It has been deleted.

Page 5, line 138: Please add a sentence saying that Vd is the dry deposition velocity.

Response: The sentence has been added following the suggestion.

Page 5, line 143: Vg and Vphor are not detailed. Please add a formula or a reference for both of them.

Response: Thanks for pointing out it. The reference (Wu et al., 2018) is added in the revised manuscript.

Reference:

Wu, M., Liu, X., Zhang, L., Wu, C., Lu, Z., Ma, P.-L., Wang, H., Tilmes, S., Mahowald, N., Matsui, H., and Easter, R. C.: Impacts of Aerosol Dry Deposition on Black Carbon Spatial Distributions and Radiative Effects in the Community Atmosphere Model CAM5, Journal of Advances in Modeling Earth Systems, 10, 1150–1171, 2018.

Page 5, line 153: It is not clear that Eg = Egb + Egt.

Response: Thanks for pointing out it. We have revised the description of Eg as Eg = Egb + Egt.

Page 5, line 159: tph+ is not detailed. Please add a reference or a formula.

Response: Thanks for pointing this out. The reference (Petroff et al., 2010) is added in the revised manuscript.

Reference:

Petroff, A. and Zhang, L.: Development and validation of a size-resolved particle dry deposition scheme for application in aerosol transport models, Geoscientific Model Development, 3, 753-769, 2010.

Page 5, line 183: Rs is not defined.

Response: Thanks for pointing out it. *Rs* is the surface resistance, which is

generally expressed as the reciprocal of the surface deposition velocity (V_{ds}). It has been defined in the equation (13) in the revised manuscript.

Page 7, line 216: What is "chem_opt(122)"?

Response: The chem_opt is an option in WRF-Chem to choose which chemical scheme is used (e.g., 10 for CBMZ/MOSAIC). We add an option 122 for users to start the CUACE chemistry module. We have rewritten the description in the revised Section 4.

Page 8, line 223: A reference is missing for KPP.

Response: The reference (Damian et al., 2002) has been added following your suggestion.

Reference:

Damian V, Sandu A, Damian M, Potra F, Carmichael G R. The kinetic preprocessor KPP-a software environment for solving chemical kinetics. Computers & Chemistry, 2002, 26(11): 1567–1579.

Page 8, line 247: The authors does not specify whether WRF is used in hydrostatic or NH mode.

Response: Thanks for pointing out it. The WRF is used in NH mode. It has been specified in the revised Section 5.1.

Page 9, line 268: Is it possible to add a figure showing the extent of the MEIC inventory? Maybe it could be added on Figure 2.

Response: Thanks for the suggestion. We added a new figure (Fig. S2) in the supplement to show the extent of the MEIC inventory, and state in the revised Section 5.1: "Figure S2 in the supplement shows the MEIC emissions of $PM_{2.5}$, NO_x, SO_2 and CO in the three years, from which it can be seen that anthropogenic emissions of $PM_{2.5}$, SO_2 and CO in mainland China reduced remarkably from 2012

to 2016.”

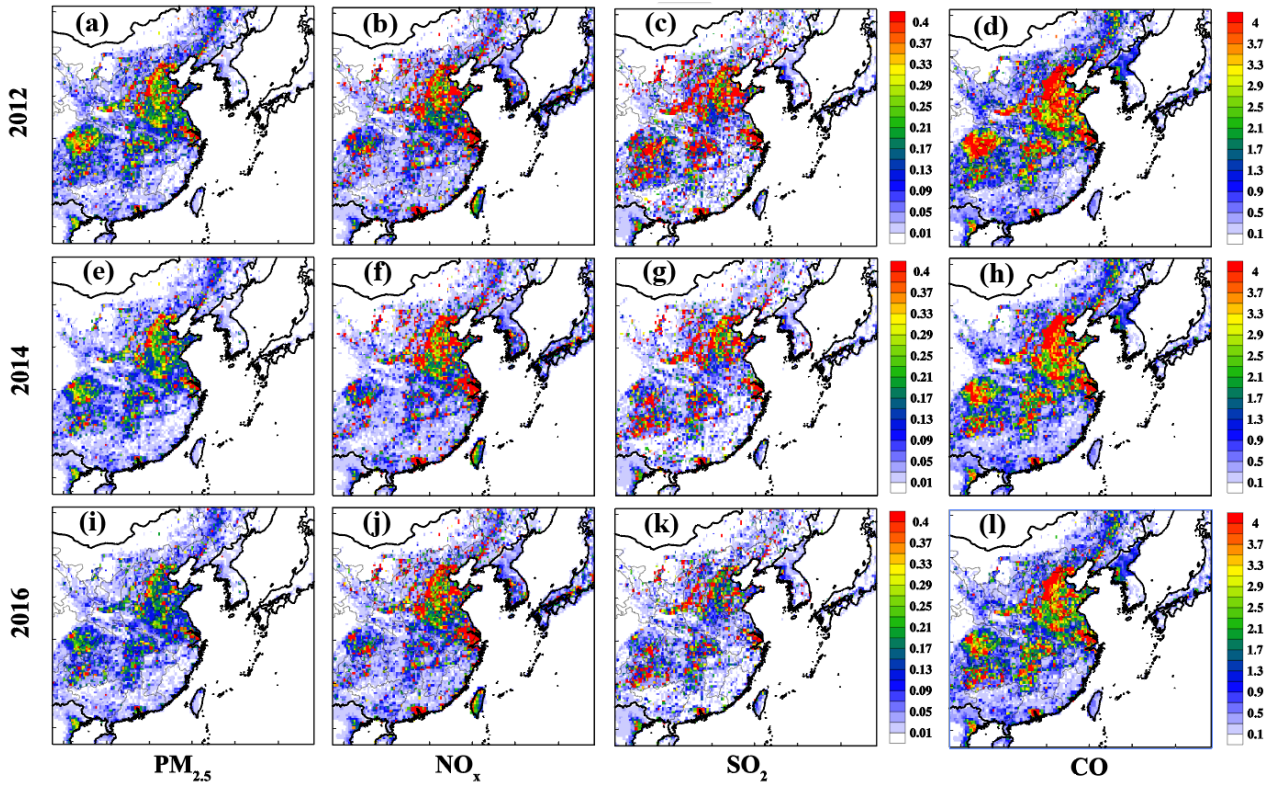

Figure S2. The MEIC emissions of $PM_{2.5}$ (a,e,i), NO_x (b,f,j), SO_2 (c,g,k), and CO (d,h,l) in the three years of (a-d) 2012, (e-h) 2014, and (i-l) 2016. Emissions outside mainland China is from the MIX emission inventory. The unit is μg m^{-2} s^{-1} for $PM_{2.5}$, NO_x, SO_2, and is mg m^{-2} s^{-1} for CO.

Page 9, line 270: Why do the authors use anthropogenic emissions representative for 2012, 2014 and 2016 to represent the years 2013, 2015 and 2017? Moreover for which year(s) is the MIX inventory representative?

Response: Currently, only the MEIC inventory representative for 2012, 2014 and 2016 is open access for download. We use anthropogenic emissions representative for 2012, 2014 and 2016 to represent the years 2013, 2015 and 2017 in order to reflect the changes in anthropogenic emissions. The year of 2010 is the MIX inventory representative for. We have explained this in the revised Section 5.1.

Page 10, line 296: Please add the mention ‘not shown’ for the time series comparison.

Response: It has been added.

Page 10, line 303: Please add a reference for the aerosol composition.

Response: Following the suggestion, the reference (Huang et al., 2014) has been added.

Reference:

Huang, R.J., Zhang, Y., Bozzetti, C., Ho, K.F., Cao, J.J., Han, Y., Daellenbach, K. R., Slowik, J. G., Platt, S. M., and Canonaco, F.: High secondary aerosol contribution to particulate pollution during haze events in China, Nature, 514, 218–222, 2014.

Page 11, line 351: Please explain what is the index of agreement exactly.

Response: The index of agreement (IOA) is based on Willmott et al. (1980), which spans between 0 (indicating "complete disagreement") to 1 (indicating "complete agreement"). It is defined as equation (R1)

$$\mathrm{IOA} = 1 - \frac{\sum_{i=1}^{n}(P_i - O_i)^2}{\sum_{i=1}^{n}(|P_i - O| + |O_i - O|)} \quad \textbf{(R1)}$$

where *P, O and i represent simulation, observation and samples, respectively.* The definition of IOA and the reference (Willmott et al., 1980) are added in the revised manuscript.

Reference:

Willmott CJ, Wicks DE. An empirical method for the spatial interpolation of monthly precipitation within California. Physical Geography 1: 59–73, 1980.

Page 11, line 351: Why do the authors only evaluate the simulations against O_3 and NO_2 observations? Indeed SO_2 observations might be a good observation since it is the direct precursor for sulfate aerosols.

Response: Thanks very much for pointing out it. We have added the evaluation of SO_2 in Section 5.2.1 in the revised manuscript following the suggestion.

Figure 3: (a), (b), (c) and (d) are missing on the figure. The 3 of mg m-3 is not in exponent size.

Response: All are revised.

Table 1: What are the value of γlow and γhigh? What is the value of RHmax? There seems to be a problem at the end of the line with a lonely bracket for the uptake coefficient for N_xO_y and SO_2.

Response: The γ_{low} and γ_{high} are the lower and upper limits of γ values. The RH_{max} is the *RH* value at which the γ reaches the upper limit. The values of γ_{low}, γ_{high} and RH_{max} are referred to the work of Zheng et al. (2015). That is, values of γ_{low} for N_2O_5, NO_2, NO_3 and SO_2 are 1E-3, 4.4E-5, 0.1 and 2E-5, respectively corresponding to the values of γ_{high} at 0.1, 2E-4, 0.23, 5E-5. The RH_{max} is 70 % for N_xO_y, and is 100 % for SO_2. Thanks for pointing this out. We have added the description γ_{low}, γ_{high} and RH_{max} in the revised Table.

Table 3: Please add "hourly" in the description of the table.

Response: It has been added.

Development of WRF/CUACE v1.0 model and its preliminary application in simulating air quality in China

Lei Zhang[1], Sunling Gong[1]*, Tianliang Zhao[2]*, Chunhong Zhou[1], Yuesi Wang[3], Jiawei Li[4], Dongsheng Ji[3], Jianjun He[1], Hongli Liu[1], Ke Gui[1], Xiaomei Guo[5,6], Jinhui Gao[7], Yunpeng Shan[8], Hong Wang[1], Yaqiang Wang[1], Huizheng Che[1], Xiaoye Zhang[1]

[1] State Key Laboratory of Severe Weather & Key Laboratory of Atmospheric Chemistry of CMA, Chinese Academy of Meteorological Sciences, Beijing, 100081, China
[2]Climate and Weather Disasters Collaborative Innovation Center, Nanjing University of Information Science &Technology, Nanjing, 210044 China
[3]State Key Laboratory of Atmospheric Boundary Layer Physics and Atmospheric Chemistry, Institute of Atmospheric Physics, Chinese Academy of Sciences, Beijing, 100029, China
[4] CAS Key Laboratory of Regional Climate-Environment for Temperate East Asia (RCE-TEA), Institute of Atmospheric Physics, Chinese Academy of Sciences, Beijing, 100029, China
[5] Heavy Rain and Drought-Flood Disasters in Plateau and Basin Key Laboratory of Sichuan Province, Chengdu, 610072, China
[6] Weather Modification Office of Sichuan Province, Chengdu, 610072, China
[7] Department of Ocean Science and Engineering, Southern University of Science and Technology, ShenZhen, 518055, China
[8] Environment and Climate Sciences Department, Brookhaven National Lab, Upton, NY, USA

Correspondence to: Sunling Gong (gongsl@cma.gov.cn) and Tianliang Zhao (tlzhao@nuist.edu.cn)

Abstract. The development of chemical transport models with advanced physics and chemical schemes could improve air-quality forecasts. In this study, the China Meteorological Administration Unified Atmospheric Chemistry Environment (CUACE) model, a comprehensive chemistry module incorporating gaseous chemistry and a size-segregated multicomponent aerosol algorithm, was coupled to the Weather Research and Forecasting (WRF)-Chem framework using an interface procedure to build the WRF/CUACE v1.0 model. The latest version of CUACE includes an updated aerosol dry deposition scheme and the introduction of heterogeneous chemical reactions on aerosol surfaces. We evaluated the WRF/CUACE v1.0 model by simulating $PM_{2.5}$, O_3, ~~and~~ NO_2 and SO_2 concentrations for January, April, July, and October (representing winter, spring, summer, and autumn, respectively) in 2013, 2015, and 2017 and comparing them with ground-based observations. Secondary inorganic aerosol simulations for North China Plain (NCP), Yangtze River Delta (YRD), and Pearl River Delta (PRD) were also evaluated ~~through a simulation of a heavy haze pollution event during 9–15 January 2019 in the North China Plain~~. The model well captured the variations of $PM_{2.5}$, O_3, and NO_2 concentrations in all seasons in eastern China. However, it is difficult to accurately reproduce the variations of air pollutants over Sichuan Basin (SCB), due to its deep basin terrain. The simulations of SO_2 were generally reasonable in the NCP and YRD with the bias at -15.5 % and 24.55 %, respectively, while poor in the PRD and SCB. The sulfate and nitrate simulations ~~are~~ were substantially improved by introducing heterogenous chemical reactions into the CUACE model (e.g., change in bias from −95.0% to 4.1% for sulfate and from 124.1% to 96.0% for nitrate in the NCP). Additionally, The

Formatted: Superscript
Formatted: Superscript
Formatted: Subscript
Formatted: Subscript

WRF/CUACE v1.0 model was revealed with better performance in simulating chemical species relative to the coupled Fifth-Generation Penn State/NCAR Mesoscale Model (MM5)-CUACE model. The development of the WRF/CUACE v1.0 model represents an important step towards improving air-quality modelling and forecasts in China.

1 Introduction

The atmosphere is an extremely complex reaction system in which a large number of chemical and physical processes occur at every moment. Numerical modelling has become an effective means to study atmospheric environmental changes and their mechanisms due to its capability at large spatial-temporal scales and with high resolution. Against the continuing rapid increase in fine particle pollution in China, chemical transport models (CTMs) have been developed in recent years and new physical and chemical atmospheric mechanisms have been presented, for instance, heterogenous chemical reactions, the production of secondary organic and inorganic aerosols, and dry deposition schemes. However, some of the mechanisms have yet to be well parameterized into CTMs for air-quality forecasts in China. Numerical modelling in combination with field observations and laboratory analyses is constantly improving our understanding of atmospheric physical and chemical processes. There is an urgent need to develop and improve CTMs to provide more powerful tools for studying the atmospheric environment, in particular for the mitigation of fine particle pollution in China.

Meteorological conditions is accepted as one of the main factors affecting atmospheric chemical processes and the aerial transport of noxious materials, and, in turn, chemical species can impact meteorological conditions by radiation feedback and cloud formation (Grell and Baklanov, 2011). Historically, CTMs were developed separately from meteorological models owing to the complexity of the atmosphere and the economics of computer calculations. Thus, CTMs were generally driven by meteorological datasets from a pre-run of the meteorological model. Information about the rapid meteorological processes, such as changes in wind direction and speed or the planetary boundary layer, are barely recorded by the low-temporal-resolution meteorological outputs (typically once or twice per hour), which may impact the accuracy of the air-quality forecasts. Coupled systems that realize the synchronous integration and two-way interactions of meteorology and chemistry are an important development for the traditional CTM approach to air-quality forecasting and there have been many endeavors devoted to this (Jacobson et al., 1996; Lin et al., 2020; Lu et al., 2020; Zhang et al., 2010).

To tackle serious air pollution in China and East Asia, with a particular focus on haze pollution

forecasting, the China Meteorological Administration (CMA) has been developing the Chinese Unified Atmospheric Chemistry Environment (CUACE) model, a chemistry module that can be driven by meteorological models. The CUACE has been integrated into the Fifth-Generation Penn State/NCAR Mesoscale Model (MM5) and the mesoscale version of the Global/Regional Assimilation and Prediction System (GRAPES, a meteorological model developed by CMA) to build a fog-haze forecasting system (An et al., 2016; Wang et al., 2015a; Zhou et al., 2012). Both of these coupled systems have been running operationally at national and provincial meteorological administrations since 2014, and have been used for air-quality assurance for many major events in China. However, active development of the MM5 model ended with version 3.7.2 in 2005, and it has been largely superseded by the Weather Research and Forecasting (WRF) model (Skamarock, 2008). The WRF model has been shown to have a better performance relative to the MM5 model due to its better numerical dynamic core and greater number of physical parameterization schemes, and it is now used as a host model for coupling with different CTMs for scientific research and air-quality forecasting, such as the WRF-Chem and WRF-CMAQ models (Grell et al., 2005; Wong et al., 2012). The WRF model has also been used to provide pre-run meteorological fields to drive models such as CAMx and FLEXPART, as well as to provide boundary and initial fields for local-scale models. Therefore, it is important to develop the CUACE module by coupling it with state-of-the-art meteorological models.

The chemical reaction mechanisms in the CUACE module, as well as in current CTMs, are proposed under clean conditions. In the context of composite air pollution in China, particularly during severe haze episodes with a rapid increase in fine particles ($PM_{2.5}$), their applicability needs to be improved. Heterogenous chemical reactions, mechanisms missing in current models, were revealed as a crucial factor to explain the dramatic increase of $PM_{2.5}$ during hazy days (Zheng et al., 2015), such as the heterogenous uptake of dinitrogen pentoxide at night (Wang et al., 2017), and the heterogeneous oxidation of dissolved SO_2 by NO_2 (Gao et al., 2016; Seinfeld and Pandis, 2012). Another process focused on here is the dry deposition of particles, where the difference between model predictions and field measurements appears greatest for vegetated canopies and for the accumulation size range of airborne particles. Ongoing research is investigating the factors that give rise to this discrepancy and providing new approaches to predicting the deposition (Hicks et al., 2016). However, few studies have incorporated these mechanisms into 3D CTMs (Wu et al., 2018).

The objectives of this study were to develop the CUACE module from three aspects: (1) introduce heterogenous reactions and update the dry deposition scheme of particles; (2) couple the CUACE to the WRF model to build the WRF/CUACE v1.0 system; and (3) evaluate the model against observations of surface air pollutants.

2 Model description

2.1 WRF model

The Advanced Research WRF version 3 (WRF-ARW) is used to simulate meteorological processes and advection of atmospheric components in the WRF/CUACE v1.0 model. The WRF-ARW is a state-of-the-science mesoscale meteorological model, making simulations that are based on actual atmospheric conditions or idealized conditions feasible (Langkamp and Böhner, 2011). The equation set for the WRF-ARW is fully compressible, Eulerian non-hydrostatic with a run-time hydrostatic option. It is conservative for scalar variables. The prognostic variables consist of velocity components u and v in Cartesian coordinates, vertical velocity w, perturbation potential temperature, perturbation geopotential, and perturbation surface pressure of dry air, as well as several optional prognostic variables depending on the model physical options (Skamarock et al., 2008; Wong et al., 2012).

2.2 CUACE module

The CUACE is a unified chemistry module, which treats most of the physical and chemical processes, except advection and convection processes that done by its host model. The main processes treated in CUACE module include emissions, gas chemistry, dry and wet deposition, vertical mixing, aerosol-cloud interaction, and clear-air (i.e., aerosol produced by chemical transformation of their precursors together with particle nucleation, condensation and coagulation) (An et al., 2016; Zhou et al., 2012; Gong et al., 2003).

~~The CUACE module is a unified atmospheric chemistry module incorporating three major functional modules: emissions, gaseous chemistry, and a size-segregated multicomponent aerosol algorithm (Zhou et al., 2012), and has been designed as a unified chemistry module that can be coupled to any atmospheric model at various temporal and spatial scales.~~ The CUACE is typically configured with the second generation of the Regional Acid Deposition Model (RADM2) as its gas~~eous~~ chemistry module, which represents 63 species through 21 photochemical reactions and ~~121~~ 136 gas phase reactions. As the gaseous chemistry (RADM2) in the CUACE module is not computationally economic and it is hard coded, which means that it is not conducive to adapting chemical reactions in the future, the CBM-Z photochemical mechanism (Zaveri and Peters, 1999) with a better computational efficiency is added with the KPP protocol (Damian et al., 2002) to replace the RADM2 mechanism. CBM-Z mechanism contains 55 species, 114 reactions and 20 photochemical reactions. It is based on the widely used Carbon Bond Mechanism (CBM-IV) and

uses the lumped structure approach for condensing organic species and reactions. CBM-Z extends the CBM-IV to include revised inorganic chemistry, explicit treatment of the lesser reactive paraffins, methane and ethane, revised treatments of reactive paraffin, olefin, and aromatic reactions, inclusion of alkyl and acyl peroxy radical interactions and their reactions with NO_3, inclusion of organic nitrates and hydroperoxides, and revised isoprene chemistry. Currently, stratospheric chemistry is not included in the CUACE module. Species (i.e, CH_4, CO, O_3, NO, NO_2, HNO_3, N_2O_5 and N_2O) above a specified pressure level are fixed to climatological values. Between the specified pressure level and the tropopause level, the species was relaxed with a 10-day relaxation factor.

The Canadian Aerosol Module (CAM) (Gong et al., 2003) is adopted as its aerosol module. There are totally seven types of aerosols treated in CAM, i.e. black carbon, primary organic carbon, sulfates, nitrates, ammonium, soil dust, and sea salts. The sea salt emissions are calculated online using the parametrization scheme developed by Gong et al. (2003). Soil dust emissions are simulated using the Marticorena–Bergametti–Alfaro scheme (Alfaro and Gomes, 2001; Marticorena and Bergametti, 1995). With the exception of ammonium, the aerosol size spectrum is divided into 12 bins with fixed boundaries of 0.005–0.01, 0.01–0.02, 0.02–0.04, 0.04–0.08, 0.08–0.16, 0.16–0.32, 0.32–0.64, 0.64–1.28, 1.28–2.56, 2.56–5.12, 5.12–10.24, and 10.24–20.48 μm. The detailed description of aerosol physical and chemical processes in the CAM module could be found in Gong et al. (2003). ~~The multicomponent aerosols in each size bin are subject to the mass conservation equation as follows:~~

$$\frac{\partial X_{ip}}{\partial t} = \left.\frac{\partial X_{ip}}{\partial t}\right|_{TRANSPORT} + \left.\frac{\partial X_{ip}}{\partial t}\right|_{SOURCES} + \left.\frac{\partial X_{ip}}{\partial t}\right|_{CLEARAIR} + \left.\frac{\partial X_{ip}}{\partial t}\right|_{DRY} + \left.\frac{\partial X_{ip}}{\partial t}\right|_{IN-CLOUD} + \left.\frac{\partial X_{ip}}{\partial t}\right|_{BELOW-CLOUD},$$

~~where the change rate in the mixing ratio of dry particle mass constituent p within the size range i has been divided into components (or tendencies) for transport, sources, clear air, dry deposition, and in-cloud and below-cloud processes. The main aerosol processes considered in CAM include coagulation, nucleation, condensation, collision, aerosol-cloud interaction, dry deposition, and wet scavenging (An et al., 2016; Gong et al., 2003).~~

3 Development of the CUACE module

3.1 Update with particle dry deposition scheme

The CUACE module currently parameterizes particle dry deposition velocity according to the method of Zhang et al. (2001) (Z01), which tends to overestimate the dry deposition, especially for fine particles (Petroff and Zhang, 2010). In this study, we use the scheme ~~that~~ developed by Petroff and Zhang (2010) (PZ10) to replace the original scheme in the CUACE module. The most significant

Formatted: Subscript
Formatted: Subscript
Formatted: Subscript
Formatted: Subscript
Formatted: Subscript
Formatted: Subscript
Formatted: Subscript
Formatted: Subscript

difference between the Z01 and PZ10 scheme is the treatment of *Rs*, which stands for the dry velocity contributed by surface resistance, consisting of Brownian diffusion, turbulent impaction, interception and rebound. According to the study of Wu et al., (2018), dry deposition velocity of fine particles is strongly affected by the Brownian diffusion and turbulent impaction. Thereby, it could be inferred that the Z01 scheme is prone to overestimate the effect of Brownian diffusion and turbulent impaction. In a recent study by Emerson et al. (2020), with observationally constrained approach, the Z01 scheme was revised to be with weaker effect of Brownian diffusion, and as a result, got better performance in simulating the dry deposition velocity of fine particles.

Formatted: Font: Italic

Both of the Z01 and PZ10 schemes use the "resistance" analogy, but with quite different formulas. The PZ10 scheme improved the surface resistance and collection efficiency of the Z01 scheme to overcome the problem of overestimating the dry deposition velocity of fine particles. The PZ10 scheme is detailed as follows:

$$V_d = V_{drift} + \frac{1}{R_a + R_s} \quad (1)$$

Here V_d is the dry deposition velocity; V_{drift} represents drift velocity, which is equal to the sum of gravitational settling and phoretic velocity and is expressed as

$$V_{drift} = V_g + V_{phor} \quad (2)$$

where V_g is the gravitational settling velocity and V_{phor} accounts for the phoretic effects that are related to differences in temperature, water vapor, or electricity between the collecting surfaces and the air (Wu et al., 2018).

The aerodynamic resistance (R_a) and surface resistance (R_s) are calculated differently for vegetated and unvegetated surfaces. For vegetated surfaces, R_a is parameterized as

$$R_a = \frac{1}{\kappa * u_*}\left[\ln\left(\frac{z_R - d}{h - d}\right) - \Psi_h\left(\frac{z_R - d}{L_O}\right) + \Psi_h\left(\frac{h - d}{L_O}\right)\right] \quad (3)$$

where κ is the von Karman constant (0.4), u_* is the friction velocity above canopy, z_R is the reference height, h is the canopy height, d is the displacement height of the canopy, L_O is the Obhukov length, and Ψ_h is the integrated form of the stability function for heat.

Surface resistance (R_s) is generally expressed as the reciprocal of the surface deposition velocity (V_{ds}), which is parameterized as

$$V_{ds} = u_* E_g \frac{1 + \left[\frac{Q}{Q_g} - \frac{\alpha}{2}\right]\frac{tan(h\eta)}{\eta}}{1 + \left[\frac{Q}{Q_g} + \alpha\right]\frac{tan(h\eta)}{\eta}} \quad (4)$$

where $E_g = E_{gb} + E_{gt}$ is the total collection efficiency on the ground below the vegetation ~~and consists of two parts:~~ ~~(1)~~E_{gb} and E_{gt} represent Brownian diffusion ~~(E_{gb})~~ and ~~(2)~~ turbulent impaction~~,~~ respectively~~(E_{gt})~~. E_{gb} is parameterized as

$$E_{gb} = \frac{Sc^{-\frac{2}{3}}}{14.5}\left[\frac{1}{6}ln\frac{(1+F)^2}{1-F+F^2} + \frac{1}{\sqrt{3}}Arctan\left(\frac{2F-1}{\sqrt{3}}\right)\frac{2F-1}{\sqrt{3}} + \frac{\pi}{6\sqrt{3}}\right]^{-1} \quad (5)$$

where F is a function of the Schmidt number (S_c) and is parameterized as $F = Sc^{\frac{1}{3}}/2.9$. E_{gt} is expressed as

$$E_{gt} = 2.5 \times 10^{-3} C_{IT} * \tau_{p\hbar}^{+2}, \quad (6)$$

where C_{IT} is a constant taken as 0.14 and $\tau_{p\hbar}^{+}$ is a function of non-dimensional relaxation time of the particle (Petroff et al., 2010).

In equation (4), the non-dimensional timescale parameter, Q, represents the ratio of turbulent transport timescale to vegetation collection timescale, and Q_g is the analogy of Q used for the transfer to the ground. Q << 1 characterizes a situation where turbulent mixing is efficient and the transfer of particles is limited by the collection efficiency on leaves. Meanwhile, Q >>1 corresponds to a situation where particles are efficiently collected by leaves and transfer of turbulent mixing is limited. Q and Q_g are defined as:

$$Q = \frac{LAI*E_T*h}{l_{mp}(h)} \quad (7)$$

$$Q_g = \frac{E_g*h}{l_{mp}(h)} \quad (8)$$

where LAI is the two-sided leaf area index, E_T is the total collection efficiency by various physical processes, and l_{mp} is the mixing length for particles. E_T is expressed as:

$$E_T = \frac{U_h}{u_*}(E_B + E_{IN} + E_{IM}) + E_{IT} \quad (9)$$

where U_h is the horizontal mean wind speed at canopy height h; and E_{B}, E_{IN}, E_{IM}, and E_{IT} are the collection efficiencies by Brownian diffusion, interception, inertial impaction, and turbulent impaction, respectively. The term η is taken as

$$\eta = \sqrt{\frac{\alpha^2}{4}} + Q \quad (10)$$

where α is the aerodynamic extinction coefficient, and is expressed as

$$\alpha = \left(\frac{k_x*LAI}{12k^2\left(1-\frac{d}{h}\right)^2}\right)^{\frac{1}{3}} \phi_m^{\frac{2}{3}}\left(\frac{h-d}{L_O}\right) \quad (11)$$

where k_x is the inclination coefficient of the canopy elements and ϕ_{m} is the non-dimensional stability function for momentum.

For non-vegetated surfaces, the aerodynamic resistance Ra ~~Ra~~ is calculated as

$$Ra = \frac{1}{\kappa u*}\left[\ln\left(\frac{z_R-d}{z_0}\right) - \Psi_h\left(\frac{z_R-d}{L_O}\right) + \Psi_h\left(\frac{z_0}{L_O}\right)\right] \quad (12)$$

and the surface deposition velocity V_{ds} is expressed as

$$V_{ds} = u_*(E_{gb} + E_{IT}) \quad (13)$$

3.2 Introduction of heterogeneous chemistry

The study of heterogeneous chemical reactions mostly focuses on the surface of dust aerosols, but the parameterization schemes of heterogeneous chemical reactions on different types of aerosol have not been well established (Zheng et al., 2015). The following are the heterogeneous chemical reactions on aerosol surfaces that added to the CUACE module in this study ("Aerosol" in the reactions stands for all the aerosols in the model):

H_2O_2 (gas) $\xrightarrow{\text{Aerosol}}$ ~~+ Aerosol →~~ Products (14)

HNO_3 (gas) $\xrightarrow{\text{Aerosol}}$ ~~+ Aerosol →~~ $0.5NO_3^-$ + $0.5NO_x$ (gas) (15)

HO_2 (gas) + Fe(II) → Fe(III) + H_2O_2 (16)

N_2O_5 (gas) $\xrightarrow{\text{Aerosol}}$ ~~+ Aerosol →~~ 2 NO_3^- (17)

NO_2 (gas) $\xrightarrow{\text{Aerosol}}$ ~~+ Aerosol →~~ NO_3^- (18)

NO_3 (gas) $\xrightarrow{\text{Aerosol}}$ ~~+ Aerosol →~~ NO_3^- (19)

O_3 (gas) $\xrightarrow{\text{Aerosol}}$ ~~+ Aerosol →~~ Products (20)

OH (gas) $\xrightarrow{\text{Aerosol}}$ ~~+ Aerosol →~~ Products (21)

SO_2 (gas) $\xrightarrow{\text{Aerosol}}$ ~~+ Aerosol →~~ SO_4^{2-} (22)

Reactions (15) and (17)–(19) describe the formation of sulfate and nitrate on the surface of sand dust, and the other four reactions describe mineral aerosols as sinks of gaseous substances. In this study, these nine heterogeneous reactions were extended to all types of aerosol surface in the CUACE, referring to the approach of Zheng et al. (2015) for the CMAQ model. The first-order chemical kinetic equation for calculating the adsorption efficiency of a gas on an aerosol surface is:

$$\frac{dC_i}{dt} = -k_i C_i \quad (23)$$

where C_i represents the concentration of gas i and k_i is the pseudo-first-order rate constant and is supposed to be irreversible. The value of k_i is defined referring to Jacob (2000) as:

$$k_i = \left(\frac{a}{D_i} + \frac{4}{v_i \gamma_i}\right)^{-1} A \quad (24)$$

where a is the aerosol diameter, D_i is the diffusion coefficient for gas reactant i, v_i is the mean molecule speed of gas reactant i, γ_i is the uptake coefficient of the heterogeneous reaction for the gas reactant i, and A is the surface area of aerosols in unit volume air. The value of γ_i is obtained from previous laboratory studies (Table 1) and other parameters are calculated in the WRF/CUACE v1.0 model.

Formatted: Indent: First line: 0.85 cm, Don't snap to grid

Formatted: Font: 四号

Formatted: Two Lines in One

4 Coupling of the CUACE module with the WRF model

The coupling of the WRF/CUACE v1.0 model is based on the framework of WRF/Chem model and uses most of ~~the~~ its existing infrastructure ~~in the WRF-Chem model~~. WRF-Chem is a meteorology-chemistry coupled model. In the chemical module of the WRF-Chem, the processes are split to emissions, vertical mixing, dry deposition, convection, gas chemistry, cloud chemistry, aerosol chemistry and wet deposition, all of which are integrated in an interface procedure (chem_driver). Advection process is treated in the WRF model. Information, such as rainfall rates, vertical mixing coefficients and convective updraft properties, is provided by WRF to calculate the processes treated in the chemical module. WRF-Chem uses registry tools for automatic generation of application code. Physical and chemical variables, as well as options of parameterization schemes are coded in files (such as registry.chem) in the directory of WRFV3/Registry, which provides the convenience for developers to add variables and options.

Following the registry tools ~~for automatic generation of application code~~ in ~~the~~ WRF-Chem model, a registry file (registry.cuace) is written to store the chemical variables and startup option of the CUACE module ~~module, as well as a new parameter of chem_opt (122) for users to start the WRF/CUACE v1.0 model. An interface procedure, cuace_driver, was first designed to integrate the core sections of the aerosol physical and chemical processes in the CUACE module (module_ae_cam.F) with the WRF framework.~~ The flow of the major process splitting in the coupled WRF/CUACE v1.0 model is illustrated in Fig. 1 with the structure of related subroutines given in Fig. S1 in the supplement. The WRF/CUACE v1.0 model uses several modules of the original WRF/Chem model, i.e., modules of advection, vertical mixing, convection, biomass emissions, anthropogenic gas emissions, photolysis and gas dry/wet deposition (Fig. S1). As described in Section 2.2, the CBM-Z mechanism is newly added with the KPP protocol (Damian et al., 2002) to replace the RADM2 mechanism in the original CUACE module. An interface procedure, cuace_driver, is designed to integrate the core sections of the aerosol physical and chemical processes of the CUACE module with the WRF framework (Fig. S1). ~~The interface procedure is placed in the chemical interface of WRF-Chem (chem_driver). As the gas-phase chemistry (RADM2) in the CUACE model is not computationally economic and it is hard coded, which means that it is not conducive to adapting chemical reactions in the future, the CBM-Z gas chemistry mechanism with a better computational efficiency is added with the KPP (Kinetic PreProcessor) protocol as the gas chemistry mechanism of the CUACE module.~~

~~The flow of the major process splitting in the coupled WRF/CUACE v1.0 model is illustrated in Fig. 1. Process splitting in the WRF/CUACE v1.0 model is generally the same as in the WRF-Chem~~

~~model. The CUACE module is independent from the original chemical module of WRF-Chem, except that they share the same advective/convective transport scheme, anthropogenic emissions module, and the dry/wet deposition of gas species.~~

~~In the CUACE module, most of the aerosol physical and chemical processes, such as coring, collision, condensation, dry deposition, wet scavenging, and aerosol activation, are gathered to the CAM section (Fig. 1). Meteorological fields outputted from the WRF model and chemical species from the CUACE module can exchange directly through the interface procedure.~~ No spatial interpolation of the meteorological and chemical data is required as both the CUACE and the WRF models can be configured to the same gird configurations and coordinate systems. The feedback of chemical species on meteorology in the current WRF/CUACE version is not realized, but is under development and will be released in a future paper.

5 Performance of WRF/CUACE v1.0 in air-quality simulation

5.1 Model configuration

At present, there are four major polluted areas in China, namely, the North China Plain (NCP), the Yangtze River Delta (YRD), the Pearl River Delta (PRD), and Sichuan Basin (SCB). To include all these regions, the simulation area is configured as in Fig. 2. There are two domains in total. The boundary field of the inner domain is obtained by the interpolation of its outer domain. The outer region covers the whole of East Asia and its adjacent areas with a horizontal resolution of 54 km and a total of 120×110 grids centered at 30.46° N and 105.82° E. The inner region covers most of China on the east side of the Qinghai-Tibet Plateau with a horizontal resolution of 18 km and 193×175 grids. There are 32 vertical layers with the top pressure at about 100 hPa. The main physical and chemical options in the model are shown in Table 2. With WRF used in non-hydrostatic mode, ~~–~~ ~~W~~we performed two simulations. One for January, April, July, and October in three years, 2013, 2015, and 2017, to evaluate the model on a long timescale, and one for three periods during which SIA observations were conducted (i.e., ~~–~~5–16 January 2019 in Langfang, 3–29 December 2013 in Nanjing, and 1–10 January 2017 in Chengdu)~~,~~, to investigate improvements in simulating SIA with heterogenous chemistry. ~~during which intensive observations of secondary inorganic aerosols (SIA) were performed at Xianghe Site (39.798°N, 116.958°E; 15 m above sea level), which is approximately 35 km northeast of Langfang city (Fig. 2) in the NCP region, to investigate improvements in simulating SIA with heterogenous chemistry.~~

The model uses the FNL global reanalysis data of the NCEP (National Centers for

Environmental Prediction) to provide the meteorological initial and boundary fields with spatial and temporal resolution of 6 h and 1°×1°, respectively. The initial and boundary chemistry conditions are based on the vertical profiles of O_3, SO_2, NO_2, VOCs (volatile organic compounds), and other air pollutants from the NOAA Aeronomy Lab Regional Oxidant Model (NALROM) (Liu et al., 1996).

Anthropogenic emissions are derived from the MIX emission inventory representative for 2010 (http://www.meicmodel.org/dataset-mix.html) (Li et al., 2017), which is an Asian anthropogenic emissions inventory developed for the third phase of the East Asian Model Comparison Plan (MICS-Asia III) and the United Nations Hemispheric Atmospheric Pollution Transport Plan (HTAP). The inventory provides monthly grid emission data with 0.25° spatial resolution for five emission sectors (electricity, industry, civil, transportation, and agriculture), including $PM_{2.5}$, PM_{10}, nitrogen oxides (NO_x), sulfur dioxide (SO_2), carbon monoxide (CO), NH_3, black carbon (BC), organic carbon (OC), and non-methane volatile organic compounds (NMVOCs). During the simulation span from 2013 to 2017, China carried out strict air pollution control measures, which had a considerable impact on anthropogenic emissions. To make the anthropogenic emissions more suitable for the real emissions scenarios in the simulated years, the emissions in mainland China were replaced with the MEIC emissions inventory ~~in~~ representative for 2012, 2014, and 2016 to represent the emissions scenarios ~~of mainland China~~ in 2013, 2015, and 2017, respectively. Figure S2 in the supplement shows the MEIC emissions of $PM_{2.5}$, NO_x, SO_2 and CO in the three years, from which it can be seen that anthropogenic emissions of $PM_{2.5}$, SO_2 and CO reduced remarkably from 2012 to 2016.

For the vertical interpolation, we used the settings of Wang et al. (2010) and Zhou et al. (2017). The industrial emissions were allocated as 50, 30, and 20% in layers one to three of the model, respectively, and the power plant emission sources were allocated as 14, 46, 35, and 5% in model layers two to five, respectively. The emissions from transportation, residential, and agriculture were 95% and 5%, respectively, in the first and second layers of the model. Then, the inventory was distributed into hourly emissions using the monthly, weekly, and hourly profiles established by Tsinghua University (2006). VOCs released from vegetation was calculated online using the MEGAN model (Guenther, 2006).

Formatted: Subscript
Formatted: Subscript
Formatted: Subscript
Formatted: Subscript
Formatted: Subscript

5.2 Evaluation against ground-based observations

5.2.1 Meteorological evaluation

The simulated hourly temperature at 2 m (T2), hourly relative humidity at 2 m (RH2) and hourly wind speed at 10 m (WS10) were selected for evaluation. Table S1 in the supplement shows

the observation mean, simulation mean, correlation coefficient (*R*), MB, ME and RMSE of the meteorological fields in the NCP, YRD, PRD and SCB, respectively. The MB and RMSE for T2 vary from 0.48 to 1.14 °C and from 2.01 to 2.50 °C, respectively, indicating surface temperatures are slightly overestimated in the four regions. The *R* value for T2, ranging from 0.88 to 0.93, indicates the variation trends are well captured by the model. The model underestimates RH2 in the four regions with the MB ranging from -6.22 to -14.30 % and the RMSE ranging from 13.95 to 18.77 %, which are comparable with previous studies in China (Wang et al., 2014; Gao et al., 2016). The RMSE for WS10 in the four regions vary from 1.47 to 1.61 m s^{-1}, fall within the "good" model performance criteria (little than 2 m s^{-1}) proposed by Emery et al. (2001). However, it should be noted that the *R* for WS10 in the SCB is relatively poor, indicating the variation trends were not well captured. The simulations of T2 and RH2 in the SCB are relatively poor than other regions as well. For example, the *R*, MB and RMSE values of T2 in the SCB are 0.88, 1.52 °C and 2.50 °C, respectively, while the values in the other three regions vary from 0.91 to 0.93, 0.48 to 1.14 °C and 2.01 to 2.39 °C. Generally, the model performed best in the YRD, followed by the PRD and NCP, and performed worst in the SCB for meteorological fields.

Formatted: Font: Italic

Formatted: Font: Italic

Formatted: Superscript

Formatted: Font: Italic

Formatted: Font: Italic

5.2.2 Chemical evaluation

Formatted: Font: Bold

Formatted: Font: Bold

Formatted: Indent: First line: 0 ch, Space Before: 24 pt, After: 12 pt

In view of the spatial-temporal differences in the haze pollution that occur in the four different regions (i.e. NCP, YRD, PRD, and SCB), here we assessed surface $PM_{2.5}$, O_3, ~~and~~ NO_2 and SO_2 simulated in the WRF/CUACE v1.0 model by region and season. Figure 3 presents a comparison of the modelled and observed daily mean $PM_{2.5}$ concentrations in spring, summer, autumn, and winter in the four regions. Overall, the WRF/CUACE v1.0 model well captured the variations in the $PM_{2.5}$ concentration, but with different performance in different regions and seasons. The correlation coefficients (*R*) for the NCP, YRD, and PRD are mostly above 0.60 and passed the 99% significance test. The *R* value between the YRD and PRD is the highest (generally higher than 0.65), followed by the NCP. The NCP, YRD, and SCB simulations in autumn and winter are generally better than that in spring and summer according to the *R* values, while that in the PRD is the opposite with a better performance during spring and summer seasons. The simulations are relatively poor in the SCB, where the complex terrain poses great challenges to meteorological field simulations (Table S1 in the supplement).

Formatted: Subscript

It is noteworthy that the WRF/CUACE v1.0 model systematically underestimated the daily $PM_{2.5}$ concentrations in the NCP when it exceeded about 200 μg m^{-3}, which mostly happened during winter (Fig. 4a). By comparing the time series of observations and simulations (not shown), we

found that the underestimation mainly occurred in the period of heavy haze pollution in some cities (such as Shijiazhuang, Hengshui, Handan, etc.). Two factors might be responsible for this. One is the uncertainty of emission sources. The formulation of an accurate emissions source inventory is always a difficult problem, especially in China. In the NCP, the seasonal difference in emission sources is substantial. A large number of unorganized loose coal combustion emissions during the winter heating season cannot be promptly accounted for by the emissions source inventory system, which increases the uncertainty of the local emission sources. The other factor might be problems in the chemical reaction mechanisms. The haze pollution study found that $PM_{2.5}$ was mainly composed of secondary particulate matter, including sulfate, nitrate, ammonium salt, and SOA (Huang et al., 2014). During heavy haze episodes, the concentration of sulfate increased substantially, but its formation mechanism remains not well recognized. The main international atmospheric chemical models (such as CMAQ, WRF-Chem, CAMx, etc.) are also found to be not ideal enough to simulate sulfate and SOA during heavy haze pollution in North China. Zheng et al. (2015) and Gao et al. (2016) initially added SO_2 heterogeneous processes in the CMAQ and WRF-Chem models, and the simulation results of sulfate improved. Although heterogeneous chemical reaction mechanisms are introduced in this study, the simulation effect of sulfate needs to be further evaluated, and the simulation of SOA is more challenging, involving thousands of VOC species and determination of their saturation, atmospheric oxidation, free radicals, acidity, and basicity. The development of a volatility basis set (VBS) is a major breakthrough that treats the organic gas/particle partitioning with a spectrum of volatilities using a saturation vapor concentration as the surrogate of volatility (Ahmadov et al., 2012; Donahue et al., 2006; Wang et al., 2015b).

The WRF/CUACE v1.0 model was further evaluated using hourly $PM_{2.5}$ concentrations and *R*, mean bias (MB), mean error (ME), normalized mean bias (NMB), normalized mean error (NME), mean fractional bias (MFB), and mean fractional error (MFE) (Table 3). As can be seen from Table 3, the correlation coefficients *R* for the NCP, YRD, PRD, and SCB are 0.59, 0.71, 0.68, and 0.59, respectively, all of which passed the 99% significance test. The YRD has the best correlation, followed by the PRD. MB values reflect that the performance of the model is reasonable in all regions, among which those in NCP and PRD are the best, with the MB values reaching −5.0 and 5.3 ~~ug~~μg m^{-3}, respectively. However, the MB values show that the simulated concentration of $PM_{2.5}$ in NCP during winter is generally underestimated by 45 ~~ug~~μg m^{-3} and overestimated by 33.9 μg m^{-3}. The dramatic positive bias in summer in the NCP is mainly due to the uncertainty in anthropogenic emissions. It is known that $PM_{2.5}$ concentration is mainly driven by primary emissions, meteorology and chemical reactions. Table S2 in the supplement shows the statistical metrics for hourly meteorological fields in winter and summer in the NCP. It can be seen that the bias of summer

Formatted: Subscript

meteorological fields is reasonable, and is comparable to those in winter (Table S2) as well as to those in the YRD and PRD (Table S1), which indicate bias in meteorological fields is not the reason. Additionally, In the YRD and PRD, where the uncertainties of anthropogenic emissions are generally known as less than that of NCP, the bias of $PM_{2.5}$ between winter and summer are comparable (Table 3), implying chemical formation of $PM_{2.5}$ in summer is not overestimated by the WRF/CUACE v1.0 model.~~.~~

Formatted: Subscript

Formatted: Subscript

From the point of view of relative deviation, the overall level of standard mean deviation NMB in the NCP is slightly better than that in the YRD and PRD, but the seasonal difference is significant, and the NMB values of the latter two (especially in the PRD) are more uniform in different seasons, maintaining at about 20%, indicating that the simulation level of the model is relatively stable in the region. The NMB of SCB is 12.2%, which is similar to that of NCP with a significant seasonal difference (11.5% in winter and 60.4% in summer). The NMBs in the NCP, YRD and PRD are basically the same, about 45%, slightly better than 50.3% in SCB.

Morris et al. (2005) provided a reference standard for MFB and MFE using hourly concentrations of simulated and observed $PM_{2.5}$. The simulation performance is identified to be excellent when MFB < 15% and MFE < 35%, identified to be good when MFB < 30% and MFE < 50%, and identified to be average when MFB < 60% and MFE < 75%, which are marked as bold, normal, and italic font, respectively, in Table 3. It can be seen that simulations in the YRD and PRD fall within the good level with the MFB/MFE reaching 21.1/42.9% and 8.6/40.1%, respectively. Both reached excellent levels in winter, which are 8.5/34.1% and 5.5/34.4%. respectively, indicating that the WRF/CUACE v1.0 model accurately captures the hourly variations of $PM_{2.5}$ in the two regions. In the NCP region, the model still maintains a good simulation level (3.3/49.1%) in the area, with obvious overestimates in summer but still maintaining an average level (44.9/56.3%). The SCB region as a whole is at the average level (20.7/51.4%). The simulation of winter and spring is better than that of spring and summer. The reason why the simulation in SCB is relatively poor is that its topography is complex, which leads to inaccurate simulation of meteorological fields and further affects the simulation of chemical species. In addition, the uncertainty of emission sources over there is also a major factor (Zhang et al., 2019).

As a whole, the seven statistical error indicators *R*, MB, ME, NMB, NME, MFB, and MFE in the four regions reached 0.63 (99% significance test), 2.7 ~~ug~~μg m^{-3}, 33.3 ~~ug~~μg m^{-3}, 2.8 %, 46.8 %, 10.6 %, and 46.2%, respectively, which showed that the WRF/CUACE v1.0 model can reasonably reproduce the changes in $PM_{2.5}$.

Statistical metrics for O_3, ~~and~~ NO_2 and SO_2, including index of agreement (IOA, see its definition in the supplement) (Willmott et al., 1980), NMB, and *R*, are shown in Table 4, along with a

Formatted: Subscript

benchmark derived from the EPA (2005, 2007). In general, the *R* values of O_3 and NO_2 in the four regions are about 0.6, which pass the 99% significance test. For O_3, NMBs indicate that the concentrations in the NCP, YRD, and PRD were well reproduced by simulations. The high consistency of the time series between the simulations and measurements was also reflected by the high values of IOA (>0.8). It should be noted that the NMB indicates that the O_3 concentrations in SCB were overestimated, which is also reflected in the scatter plot (Fig. 4d), partially due to the relatively poor simulation of meteorological fields (Table S1). ~~The complex topography and uncertainties in the emissions inventory might be responsible.~~ As the precursor of O_3, simulation of NO_2 over the NCP, YRD, PRD, and SCB was acceptable, with the NMBs all falling within the benchmark and IOAs greater than 0.70. In general, the statistical metrics for O_3 and NO_2 are comparable with other studies (Gao et al., 2018; Hu et al., 2016). The variations of SO_2 in NCP and YRD were generally reproduced by the model with bias at -15.5 % and 24.55 %, respectively. However, in the PRD and SCB, SO_2 concentrations were substantially overestimated (Table 4 and Fig. 4k-l). As previous studies revealed, emissions of SO_2 in eastern China were overestimated by national emission inventories (Zhang et al., 2018; Zhou et al., 2019; Gao et al., 2016), which might partially contribute to the overestimation of SO_2 in YRD and PRD.

Formatted: Subscript

Formatted: Subscript

Formatted: Subscript

Formatted: Subscript

On the basis of the above analysis results, the simulation results are satisfactory, with the exception of SCB.

5.3 Evaluation of SIA simulations with heterogeneous chemical reactions

Heterogeneous chemical reactions have been shown to have important effects on the formation of SIA~~s~~, especially during severe haze events with high humidity (Li et al., 2011; Wang et al., 2006; Zhao et al., 2013). The ground observations of SIA from 5 to 16 January 2019 in Langfang (NCP), from 3 to 29 December 2013 in Nanjing (YRD), and from 1 to 10 January 2017 in Chengdu (SCB) were collected for the evaluation of SIA simulations. Following the model configurations in Section 4.2, we performed WRF/CUACE v1.0 simulations with (Exp_WH) and without (Exp_WoH) heterogenous chemistry on the three periods~~for a severe haze event that occurred on 9–15 January 2019~~.

Figure 5 illustrates the hourly variations of observed SIA concentration from the Exp_WH and Exp_WoH experiments. For Langfang site, ~~T~~the simulation without heterogenous chemistry (Exp_WoH) barely capture the sulfate increase (Fig. 5a). This was substantially improved when heterogenous chemistry was included (Exp_WH), although some observed peak values are not well captured, such as those on 14 January. The overestimation of nitrate was also improved, with the

NMBs changing from 124.1% to 96.0% (Fig. 5b). It should be noted that the responses of sulfate and nitrate to heterogenous chemistry are inverse, which might be attributed to the complex thermodynamic processes of SIA formation (Zheng et al., 2015). Sulfate and nitrate will compete for ammonium, which is now the only cation currently in the CUACE model, resulting in less ammonium nitrate and more ammonium sulfate because of the more thermodynamically stable features of ammonium sulfate. As a result of the dramatical increase in sulfate in Exp_WH, the ammonium concentrations slightly increase relative to that in Exp_WoH to achieve anion–cation balance, which leads to more overestimations in the Exp_WH experiment (Fig. 5c). For Nanjing and Chengdu site, the underestimation of sulfate (Fig. 5d and 5g) and overestimation of nitrate (Fig. 5e and 5h) were also improved to varying degrees, with bias of sulfate changing from −95.3 % to -68.4 % in Nanjing and from -88.7 % to -80.1 % in Chengdu and the bias of nitrate changing from 83.0 % to 54.6 % in Nanjing and from 67.6 % to 23.5 % in Chengdu. Nonetheless, deviations in SIA simulations are still too large to neglect in those regions.

5.4 Comparison between the MM5/CUACE model and the WRF/CUACE v1.0 model

It is necessary to compare the MM5/CUACE model with the new WRF/CUACE model for the purpose of assessing the viability of the newly developed model. To this end, a simulation was performed using the MM5/CUACE model for a winter month, i.e., January 2013, during which a long-lasting haze event occurred in central and eastern China. The domain setting, anthropogenic emission inventory, initial and boundary fields of meteorology and chemistry are as the same as those of the WRF/CUACE in section 5.1. It should be known that the gas-phase chemistry mechanism and particle dry deposition scheme in MM5/CUACE model is RADM2 and Z01, respectively, that updated to CBM-Z and PZ10 in the new WRF/CUACE model. Physical parameterization used in the MM5/CUACE is shown in Table S3 in the supplement.

Figure 6 presents a comparison of the modelled and observed daily concentrations of $PM_{2.5}$, O_3, NO_2 and SO_2 in the four regions. It can be seen that the concentrations of $PM_{2.5}$, NO_2 and SO_2 simulated in WRF/CUACE are closer to the observations relative to those of MM5/CUACE model (change in bias from -23.0 % to -19.2 % for $PM_{2.5}$, from 14.7 % to -2.4 % for NO_2 and from -46.2 % to -37.5 % for SO_2). The daily variations of the three species are also relatively better captured by the WRF/CUACE model (reflected by the *R* values changing from 0.45 to 0.62 for $PM_{2.5}$, from 0.41 to 0.49 for NO_2 and from 0.19 to 0.32 for SO_2). For O_3, the differences of statistical metrics between the two models are not obvious. The MM5/CUACE model performed with a slightly smaller bias of -10.7 %

Formatted: Font: 小四, No underline
Formatted: Font: 小四, No underline
Formatted: Font: 小四, Not Bold, No underline
Formatted: Indent: First line: 2 ch, Space Before: 0 pt
Formatted: Indent: First line: 2 ch, Space Before: 0 pt, After: 0 pt, Line spacing: 1.5 lines

but with a lower R value of 0.50, which are 14.3 % and 0.55, respectively in the WRF/CUACE simulation. In summary, the new WRF/CUACE model performed better than the MM5/CUACE model in simulating air pollutants.

Formatted: Font: Not Bold

6 Summary and future work

This study develops the chemical module CUACE by adding heterogenous chemical reactions and introducing a particle dry deposition scheme developed by Petroff and Zhang (2010). The CUACE module is then incorporated into the WRF-Chem model to build the WRF/CUACE v1.0 modelling system to take advantage of the better numerical dynamic core and the greater number of physical parameterization schemes of the WRF model compared with the MM5 model.

We perform a three-year (2013, 2015, and 2017) model simulation using the WRF/CUACE v1.0 model to evaluate its performance on reproducing surface concentration variations of $PM_{2.5}$, O_3, and NO_2, which are now the main pollutants in China. A heavy haze pollution event that occurred during 9–15 January 2019 in the NCP is also selected to evaluate the SIA simulations compared with intensive ground SIA observations. The results show that WRF/CUACE v1.0 can well capture the daily and hourly variations of $PM_{2.5}$, especially in the YRD and PRD regions throughout the three years. For the NCP in winter, observed high concentrations larger than 200 μg m^{-3} are not well reproduced, which might be mainly due to uncertainties in the emissions inventory and the lack of some chemical reactions in the model. For NO_2 and O_3, the model shows small biases in the NCP, YRD, and PRD regions with correlation coefficients all larger than 0.60 and the NMBs all fall within the EPA benchmark (2005, 2007). The model shows relatively notable biases in the SCB region compared with the NCP, YRD, and PRD regions for the three pollutants, which may be mainly due to the complex terrain in the SCB (Zhang et al., 2019) and insufficient meteorological data available for the region for assimilation in the NCEP-FNL reanalysis data. ~~The Exp_WH experiment significantly improves the hourly variations in the sulfate concentration, implying a notable contribution of heterogenous chemistry to heavy haze pollution in the NCP region. Nitrate formation is restricted in the Exp_WH experiment due to the drastic increase in sulfate, which will compete for ammonium with the nitrate~~ Simulations of SIA are generally improved, especially for sulfate in the NCP. However, large uncertainties remain in the mechanisms of the heterogenous chemical reactions in the model, such as the determination of the uptake coefficients, which is based on previous studies on dust surfaces.

There are still several limitations in the current version of the WRF/CUACE v1.0 model that need to be addressed in future development. The feedback of particles, which can be divided into

direct and indirect effects, is recognized to be crucial in online coupled models, especially during periods with high particle loading. Currently in the WRF-Chem model, the direct effects of aerosols are processed following the methodology described by Ghan et al. (2001). Our future work will first focus on implementing the direct effects of aerosols, i.e. radiation feedback, following the Mie calculation to realize the direct aerosol forcing. The second step is to implement the VBS scheme to add the missing processes of SOA, which has been implied to be a main cause in the underestimation of OA formation (Gao et al., 2017; Heald et al., 2005; Spracklen et al., 2011). Although the original particle dry deposition scheme is updated with that developed by Petroff and Zhang (2010), it is difficult to evaluate whether the dry deposition process is improved as the limited technology of dry deposition observations restricts direct observations of particle dry deposition. With the observed $PM_{2.5}$ concentrations, model improvements with and without the updated dry deposition scheme are preliminary evaluated (Figure S3 in the supplement). With regards to particle dry deposition, our aim is to implement several schemes in the CUACE module, such as the schemes developed by Emerson et al. (2020), Zhang and He (2014), Zhang and Shao (2014), and Kouznetsov and Sofiev (2012), to evaluate uncertainties in the schemes on aerosol simulation, which might help the development of the particle dry deposition scheme.

Formatted: Subscript

Code availability

The WRF/CUACE v1.0 model is open-source and can be accessed at a DOI repository https://doi.org/10.5281/zenodo.3872620. All source code and data can also be accessed by contacting the corresponding authors Sunling Gong (gongsl@cma.gov.cn) and Tianliang Zhao (tlzhao@nuist.edu.cn).

Competing interests

The authors declare no competing interests.

Author Contributions

Sunling Gong, Tianliang Zhao, Hong Wang, Huizheng Che and Xiaoye Zhang led the project. Lei Zhang, Sunling Gong, Chunhong Zhou and Hongli Liu developed the model code, with assistance from Jiawei Li, Jianjun He, Ke Gui and Yaqiang Wang. Lei Zhang performed the simulations and wrote the manuscript with suggestions from all authors. Yuesi Wang ~~and~~, Dongsheng Ji and Xiaomei Guo provided the data of secondary inorganic aerosols. Jinhui Gao and Yunpeng Shan contribute to data processing. All authors contributed to the discussion and improvement of the manuscript.

Acknowledgements

This work is supported by the National Key Foundation Study Developing Programs (No. 2019YFC0214601), National Natural Science Foundation of China (No. 91744209, 41975131, 41705080), and the CAMS Basis Research Project (No. 2020Y001). We gratefully acknowledge the Atmosphere Sub-Center of Chinese Ecosystem Research Network (SCAS-CERN) for providing the data of secondary inorganic aerosols, and thank Prof. Leiming Zhang (Air Quality Research Division, Science and Technology Branch, Environment Canada) for sharing the code of aerosol dry deposition scheme.

References

Ahmadov, R., McKeen, S., Robinson, A., Bahreini, R., Middlebrook, A., De Gouw, J., Meagher, J., Hsie, E. Y., Edgerton, E., and Shaw, S.: A volatility basis set model for summertime secondary organic aerosols over the eastern United States in 2006, Journal of Geophysical Research: Atmospheres, 117, 2012.

Alfaro, S. C. and Gomes, L.: Modeling mineral aerosol production by wind erosion: Emission intensities and aerosol size distributions in source areas, Journal of Geophysical Research: Atmospheres, 106, 18075-18084, 2001.

An, X. Q., Zhai, S. X., Jin, M., Gong, S., and Wang, Y.: Development of an adjoint model of GRAPES–CUACE and its application in tracking influential haze source areas in north China, Geoscientific Model Development, 9, 2153-2165, 2016.

Bian, H. and Zender, C. S.: Mineral dust and global tropospheric chemistry: Relative roles of photolysis and heterogeneous uptake, Journal of Geophysical Research: Atmospheres, 108, 2003.

Chen, F. and Dudhia, J.: Coupling an advanced land surface–hydrology model with the Penn State–NCAR MM5 modeling system. Part I: Model implementation and sensitivity, Monthly weather review, 129, 569-585, 2001.

Chou, M.-D. and Suarez, M. J.: An efficient thermal infrared radiation parameterization for use in general circulation models, 1994.

Damian V, Sandu A, Damian M, Potra F, Carmichael G R. The kinetic preprocessor KPP-a software environment for solving chemical kinetics. Computers & Chemistry, 26(11), 1567–1579, 2002.

Donahue, N., Robinson, A., Stanier, C., and Pandis, S.: Coupled partitioning, dilution, and chemical aging of semivolatile organics, Environmental science & technology, 40, 2635-2643, 2006.

Emery, C., Tai, E., and Yarwood, G.: Enhanced meteorological modeling and performance evaluation for two Texas ozone episodes, in: Prepared for the Texas Natural Resource Conservation Commission, ENVIRON International Corporation, Novato, CA, USA, 2001.

Emerson, E. W., Hodshire, A. L., DeBolt, H. M., Bilsback, K. R., Pierce, J. R., McMeeking, G. R., and Farmer, D. K.: Revisiting particle dry deposition and its role in radiative effect estimates, Proceedings of the National Academy of Sciences, doi: 10.1073/pnas.2014761117, 2020. 202014761, 2020.

EPA, U. S.: Guidance on the Use of Models and Other Analyses in Attainment Demonstrations for the 8-hour Ozone NAAQS, EPA-454/R-405-002, 2005.

EPA, U. S.: Guidance on the Use of Models and Other Analyses for Demonstrating Attainment of Air Quality Goals for Ozone, PM2:5, and Regional Haze, EPA-454/B-407-002, 2007.

Gao, C. Y., Tsigaridis, K., and Bauer, S. E.: MATRIX-VBS (v1.0): implementing an evolving organic aerosol volatility in an aerosol microphysics model, Geoscientific Model Development, 10, 751-764, 2017.

Gao, J., Zhu, B., Xiao, H., Kang, H., Pan, C., Wang, D., and Wang, H.: Effects of black carbon and boundary layer interaction on surface ozone in Nanjing, China, Atmospheric Chemistry and Physics, 18, 7081-7094, 2018.

Gao, M., Carmichael, G. R., Wang, Y., Ji, D., Liu, Z., and Wang, Z.: Improving simulations of sulfate aerosols during winter haze over Northern China: the impacts of heterogeneous oxidation by NO_2, Frontiers of Environmental Science & Engineering, 10, 2016.

Ghan, S., Laulainen, N., Easter, R., Wagener, R., Nemesure, S., Chapman, E., Zhang, Y., and Leung, R.: Evaluation of aerosol direct radiative forcing in MIRAGE, Journal of Geophysical Research: Atmospheres, 106, 5295-5316, 2001.

Gong, S. L., Barrie, L. A., J.-P. Blanchet, Salzen, K. v., U. Lohmann, and Lesins, G.: Canadian Aerosol Module: A size-segregated simulation of atmospheric aerosol processes for climate and air quality models 1. Module development, Journal of Geophysical Research, 108, 2003.

Grell, G. and Baklanov, A.: Integrated modeling for forecasting weather and air quality: A call for fully coupled approaches, Atmospheric Environment, 45, 6845-6851, 2011.

Grell, G. A.: Prognostic evaluation of assumptions used by cumulus parameterizations, Monthly weather review, 121, 764-787, 1993.

Grell, G. A., Peckham, S. E., Schmitz, R., McKeen, S. A., Frost, G., Skamarock, W. C., and Eder, B.: Fully coupled "online" chemistry within the WRF model, Atmospheric Environment, 39, 6957-6975, 2005.

Guenther, C.: Estimates of global terrestrial isoprene emissions using MEGAN (Model of Emissions of Gases and Aerosols from Nature), Atmospheric Chemistry and Physics, 6, 2006.

Heald, C. L., Jacob, D. J., Park, R. J., Russell, L. M., Huebert, B. J., Seinfeld, J. H., Liao, H., and Weber, R. J.: A large organic aerosol source in the free troposphere missing from current models, Geophysical Research Letters, 32, 2005.

Hicks, B. B., Saylor, R. D., and Baker, B. D.: Dry deposition of particles to canopies-A look back and the road forward, Journal of Geophysical Research: Atmospheres, 121, 14,691-614,707, 2016.

Hu, J., Chen, J., Ying, Q., and Zhang, H.: One-year simulation of ozone and particulate matter in China using WRF/CMAQ modeling system, 1foldr Import 2019-10-08 Batch 1, 2016.

Huang, R.J., Zhang, Y., Bozzetti, C., Ho, K.F., Cao, J.J., Han, Y., Daellenbach, K. R., Slowik, J. G., Platt, S. M., and Canonaco, F.: High secondary aerosol contribution to particulate pollution during haze events in China, Nature, 514, 218–222, 2014.

Jacob, D. J.: Heterogeneous chemistry and tropospheric ozone, Atmospheric Environment, 34, 2131-2159, 2000.

Jacobson, M. Z., Tabazadeh, A., and Turco, R. P.: Simulating equilibrium within aerosols and nonequilibrium between gases and aerosols, Journal of Geophysical Research: Atmospheres, 101, 9079-9091, 1996.

Janjić, Z. I.: The step-mountain eta coordinate model: Further developments of the convection, viscous sublayer, and turbulence closure schemes, Monthly weather review, 122, 927-945, 1994.

Kouznetsov, R. and Sofiev, M.: A methodology for evaluation of vertical dispersion and dry deposition of atmospheric aerosols, Journal of Geophysical Research: Atmospheres, 117, 2012.

Langkamp, T. and Böhner, J.: Influence of the compiler on multi-CPU performance of WRFv3, Geoscientific Model Development, 4, 611-623, 2011.

Li, M., Zhang, Q., Kurokawa, J.-i., Woo, J.-H., He, K., Lu, Z., Ohara, T., Song, Y., Streets, D. G., and Carmichael, G. R.: MIX: a mosaic Asian anthropogenic emission inventory under the international collaboration framework of the MICS-Asia and HTAP, Atmospheric Chemistry and Physics (Online), 17, 2017.

Li, W., Zhou, S., Wang, X., Xu, Z., Yuan, C., Yu, Y., Zhang, Q., and Wang, W.: Integrated evaluation of aerosols from regional brown hazes over northern China in winter: Concentrations, sources, transformation, and mixing states, Journal of Geophysical Research: Atmospheres, 116, 2011.

Lin, H., Feng, X., Fu, T.-M., Tian, H., Ma, Y., Zhang, L., Jacob, D. J., Yantosca, R. M., Sulprizio, M. P., and Lundgren, E. W.: WRF-GC: Online coupling of WRF and GEOS-Chem for regional atmospheric chemistry modeling, Part 1: Description of the one-way model (v1. 0), Geosci. Model Dev. Discuss, 2020, 1-39, 2020.

Lin, Y.-L., Farley, R. D., and Orville, H. D.: Bulk parameterization of the snow field in a cloud model, Journal of climate

and applied meteorology, 22, 1065-1092, 1983.

Liu, S., McKeen, S., Hsie, E. Y., Lin, X., Kelly, K., Bradshaw, J., Sandholm, S., Browell, E., Gregory, G., and Sachse, G.: Model study of tropospheric trace species distributions during PEM-West A, Journal of Geophysical Research: Atmospheres, 101, 2073-2085, 1996.

Lu, X., Zhang, L., Wu, T., Long, M. S., Wang, J., Jacob, D. J., Zhang, F., Zhang, J., Eastham, S. D., and Hu, L.: Development of the global atmospheric general circulation-chemistry model BCC-GEOS-Chem v1. 0: model description and evaluation, Geosci. Model Dev. Discuss., 2020.

Marticorena, B. and Bergametti, G.: Modeling the atmospheric dust cycle: 1. Design of a soil-derived dust emission scheme, Journal of geophysical research: atmospheres, 100, 16415-16430, 1995.

Michel, A., Usher, C., and Grassian, V.: Reactive uptake of ozone on mineral oxides and mineral dusts, Atmospheric Environment, 37, 3201-3211, 2003.

Mlawer, E. J., Taubman, S. J., Brown, P. D., Iacono, M. J., and Clough, S. A.: Radiative transfer for inhomogeneous atmospheres: RRTM, a validated correlated-k model for the longwave, Journal of Geophysical Research: Atmospheres, 102, 16663-16682, 1997.

Morris, R. E., McNally, D. E., Tesche, T. W., Tonnesen, G., Boylan, J. W., and Brewer, P.: Preliminary Evaluation of the Community Multiscale Air Quality Model for 2002 over the Southeastern United States, Journal of the Air & Waste Management Association, 55, 1694-1708, 2005.

Petroff, A. and Zhang, L.: Development and validation of a size-resolved particle dry deposition scheme for application in aerosol transport models, Geoscientific Model Development, 3, 753-769, 2010.

Phadnis, M. J. and Carmichael, G. R.: Numerical investigation of the influence of mineral dust on the tropospheric chemistry of East Asia, Journal of Atmospheric Chemistry, 36, 285-323, 2000.

Seinfeld, J. H. and Pandis, S. N.: Atmospheric chemistry and physics: from air pollution to climate change, John Wiley & Sons, 2012.

Seisel, S., Börensen, C., Vogt, R., and Zellner, R.: The heterogeneous reaction of HNO_3 on mineral dust and γ-alumina surfaces: a combined Knudsen cell and DRIFTS study, Physical Chemistry Chemical Physics, 6, 5498-5508, 2004.

Skamarock, W. C., Klemp, J. B., Dudhia, J., Gill, D. O., Barker, D. M., Wang, W., and Powers, J. G.: A description of the Advanced Research WRF version 3, National Center for Atmospheric Research Technical note, NCAR/TN-475+STR, 113pp, 2008.

Spracklen, D., Jimenez, J., Carslaw, K., Worsnop, D., Evans, M., Mann, G., Zhang, Q., Canagaratna, M., Allan, J., and Coe, H.: Aerosol mass spectrometer constraint on the global secondary organic aerosol budget, Atmospheric Chemistry and Physics, 11, 12109-12136, 2011.

Tsinghua University, 2006. Control Strategy and Measurement of PM_{10} and O_3 Pollution in Beijing City. Report to Beijng Environmental Protection Bureau, Beijing, China (in Chinese).

Wang, H., Xue, M., Zhang, X. Y., Liu, H. L., Zhou, C. H., Tan, S. C., Che, H. Z., Chen, B., and Li, T.: Mesoscale modeling study of the interactions between aerosols and PBL meteorology during a haze episode in Jing–Jin–Ji (China) and its nearby surrounding region – Part 1: Aerosol distributions and meteorological features, Atmospheric Chemistry and Physics, 15, 3257-3275, 2015a.

Wang, K., Zhang, Y., Nenes, A., and Fountoukis, C.: Implementation of dust emission and chemistry into the Community Multiscale Air Quality modeling system and initial application to an Asian dust storm episode, Atmospheric Chemistry and Physics, 12, 10209-10237, 2012.

Wang, K., Zhang, Y., Yahya, K., Wu, S.-Y., and Grell, G.: Implementation and initial application of new chemistry-aerosol options in WRF/Chem for simulating secondary organic aerosols and aerosol indirect effects for regional air quality, Atmospheric Environment, 115, 716-732, 2015b.

Wang, L., Jang, C., Zhang, Y., Wang, K., Zhang, Q., Streets, D., Fu, J., Lei, Y., Schreifels, J., and He, K.: Assessment of air

quality benefits from national air pollution control policies in China. Part II: Evaluation of air quality predictions and air quality benefits assessment, Atmospheric Environment, 44, 3449-3457, 2010.

Wang, X., Wang, H., Xue, L., Wang, T., Wang, L., Gu, R., Wang, W., Tham, Y. J., Wang, Z., Yang, L., Chen, J., and Wang, W.: Observations of N_2O_5 and $ClNO_2$ at a polluted urban surface site in North China: High N_2O_5 uptake coefficients and low $ClNO_2$ product yields, Atmospheric Environment, 156, 125-134, 2017.

Wang, Y., Zhang, Q., Jiang, J., Zhou, W., Wang, B., He, K., Duan, F., Zhang, Q., Philip, S., and Xie, Y.: Enhanced sulfate formation during China's severe winter haze episode in January 2013 missing from current models, J. Geophys. Res.-Atmos., 119, 10425–10440, doi:10.1002/2013JD021426, 2014.

Wang, Y., Zhuang, G., Sun, Y., and An, Z.: The variation of characteristics and formation mechanisms of aerosols in dust, haze, and clear days in Beijing, Atmospheric Environment, 40, 6579-6591, 2006.

Wong, D. C., Pleim, J., Mathur, R., Binkowski, F., Otte, T., Gilliam, R., Pouliot, G., Xiu, A., Young, J. O., and Kang, D.: WRF-CMAQ two-way coupled system with aerosol feedback: software development and preliminary results, Geoscientific Model Development, 5, 299-312, 2012.

Willmott CJ, Wicks DE. An empirical method for the spatialinterpolation of monthly precipitation within California. Physical Geography 1, 59–73, 1980.

Wu, M., Liu, X., Zhang, L., Wu, C., Lu, Z., Ma, P.-L., Wang, H., Tilmes, S., Mahowald, N., Matsui, H., and Easter, R. C.: Impacts of Aerosol Dry Deposition on Black Carbon Spatial Distributions and Radiative Effects in the Community Atmosphere Model CAM5, Journal of Advances in Modeling Earth Systems, 10, 1150–1171, 2018.

Zhang, J. and Shao, Y.: A new parameterization of particle dry deposition over rough surfaces, Atmos. Chem. Phys, 14, 12429-12440, 2014.

Zhang, L., Gong, S., Padro, J., and Barrie, L.: A size-segregated particle dry deposition scheme for an atmospheric aerosol module, Atmospheric Environment, 35, 549-560, 2001.

Zhang, L., Guo, X., Zhao, T., Gong, S., Xu, X., Li, Y., Luo, L., Gui, K., Wang, H., Zheng, Y., and Yin, X.: A modelling study of the terrain effects on haze pollution in the Sichuan Basin, Atmospheric Environment, 196, 77-85, 2019.

Zhang, L. and He, Z.: Technical Note: An empirical algorithm estimating dry deposition velocity of fine, coarse and giant particles, Atmospheric Chemistry and Physics, 14, 3729-3737, 2014.

Zhang, L., Zhao, T., Gong, S., Kong, S., Tang, L., Liu, D., Wang, Y., Jin, L., Shan, Y., and Tan, C.: Updated emission inventories of power plants in simulating air quality during haze periods over East China, Atmospheric Chemistry and Physics, 18, 2065-2079, 2018.

Zhang, Y. and Carmichael, G. R.: The role of mineral aerosol in tropospheric chemistry in East Asia—A model study, Journal of Applied Meteorology, 38, 353-366, 1999.

Zhang, Y., Pan, Y., Wang, K., Fast, J. D., and Grell, G. A.: WRF/Chem-MADRID: Incorporation of an aerosol module into WRF/Chem and its initial application to the TexAQS2000 episode, Journal of Geophysical Research, 115, 2010.

Zhao, X., Zhao, P., Xu, J., Meng, W., Pu, W., Dong, F., He, D., and Shi, Q.: Analysis of a winter regional haze event and its formation mechanism in the North China Plain, Atmospheric Chemistry & Physics Discussions, 13, 2013.

Zheng, B., Zhang, Q., Zhang, Y., He, K. B., Wang, K., Zheng, G. J., Duan, F. K., Ma, Y. L., and Kimoto, T.: Heterogeneous chemistry: a mechanism missing in current models to explain secondary inorganic aerosol formation during the January 2013 haze episode in North China, Atmospheric Chemistry and Physics, 15, 2031-2049, 2015.

Zhou, C.-H., Gong, S., Zhang, X.-Y., Liu, H.-L., Xue, M., Cao, G.-L., An, X.-Q., Che, H.-Z., Zhang, Y.-M., and Niu, T.: Towards the improvements of simulating the chemical and optical properties of Chinese aerosols using an online coupled model – CUACE/Aero, Tellus B, 64, 2012.

Zhou, Y., Zhao, Y., Mao, P., Zhang, Q., Zhang, J., Qiu, L., and Yang, Y.: Development of a high-resolution emission inventory and its evaluation and application through air quality modeling for Jiangsu Province, China, Atmospheric Chemistry and Physics, 17, 211-233, 2017.

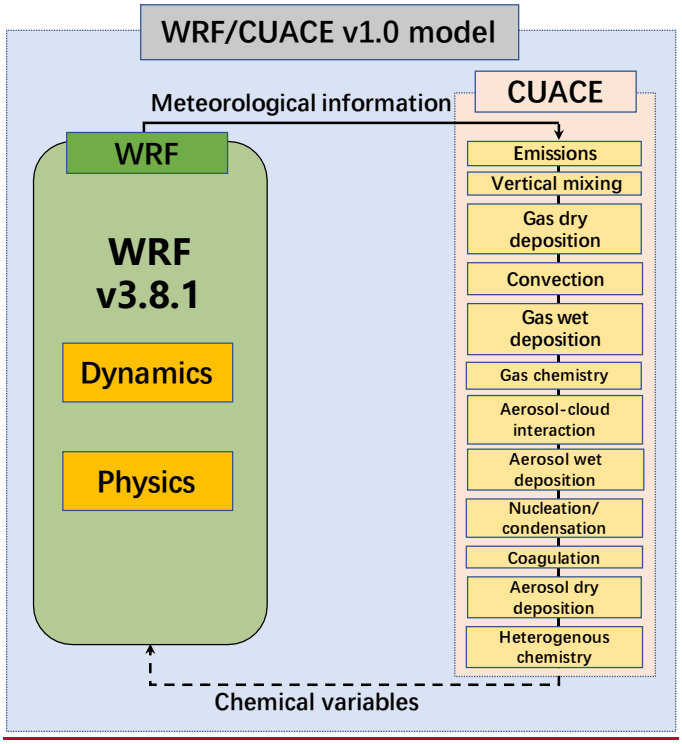
WRF/CUACE v1.0 model
Meteorological information
CUACE
WRF
WRF
v3.8.1
Dynamics
Physics
Emissions
Vertical mixing
Gas dry deposition
Convection
Gas wet deposition
Gas chemistry
Aerosol-cloud interaction
Aerosol wet deposition
Nucleation/ condensation
Coagulation
Aerosol dry deposition
Heterogenous chemistry
Chemical variables

750

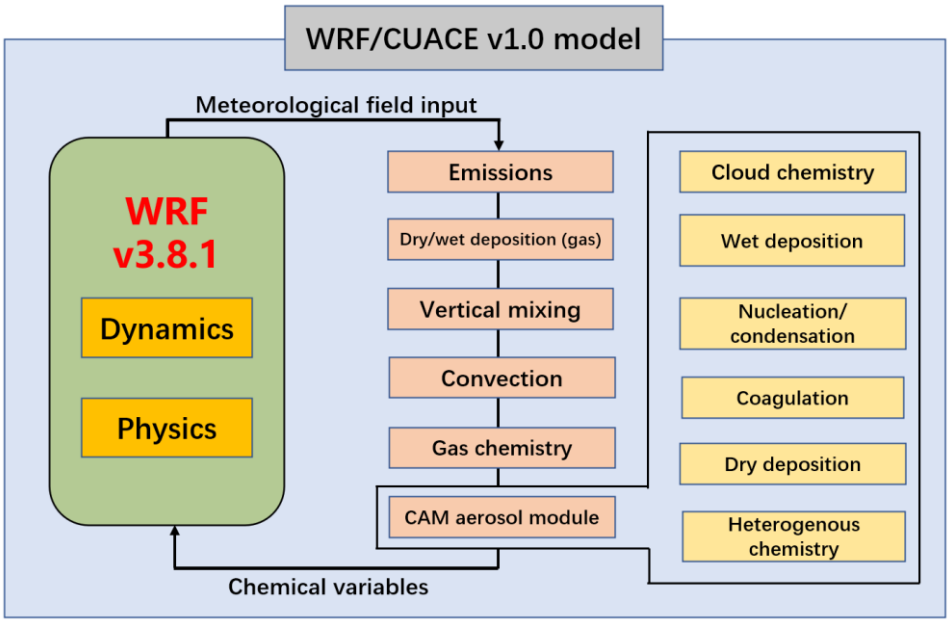

Figure 1. Schematic of modules in the WRF/CUACE v1.0 system.

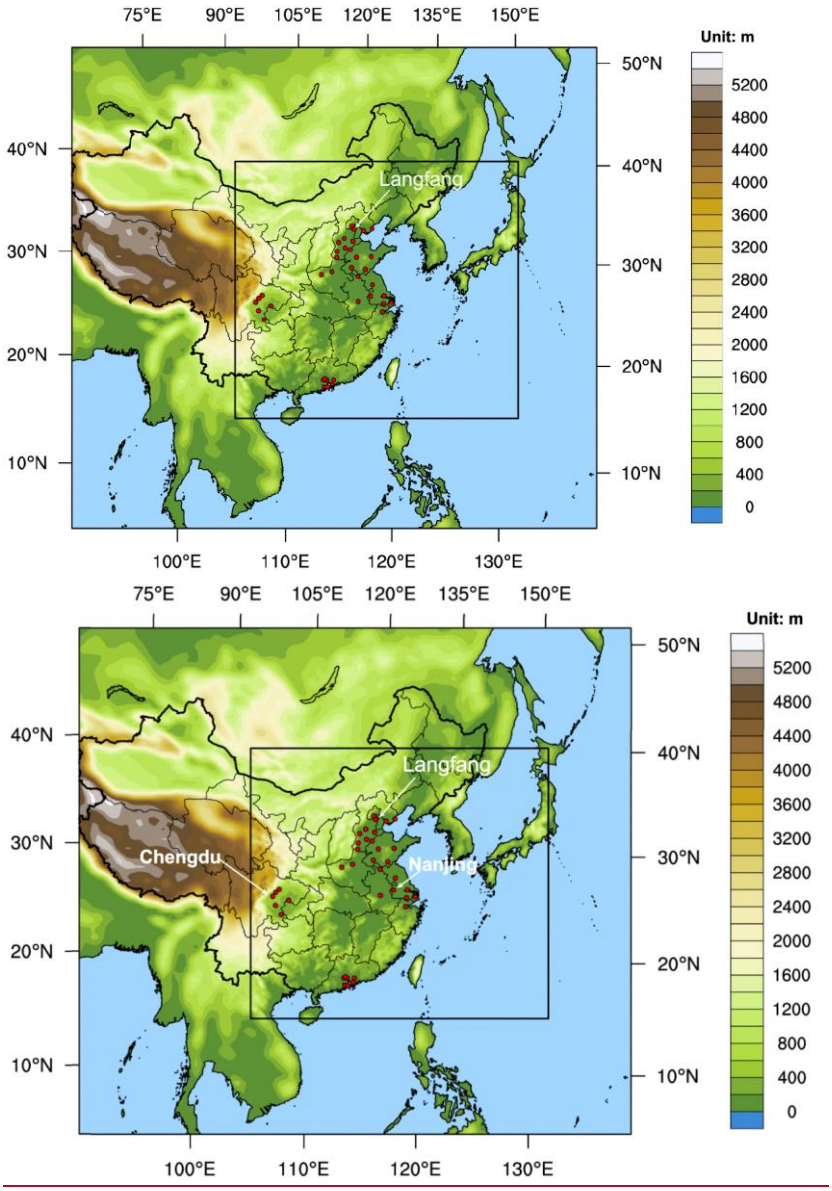

Figure 2. Model domains with the terrain distribution. Red circles indicate the cities where the surface observations of air pollutants are used for model evaluation. The ~~, and Langfang indicates that a nearby station (Xianghe site) conducted intensive SIA observation during January 2019.~~ Langfang, Nanjing and Chengdu sites marked in this figure indicate where the SIA observations are collected for evaluation of SIA simulations.

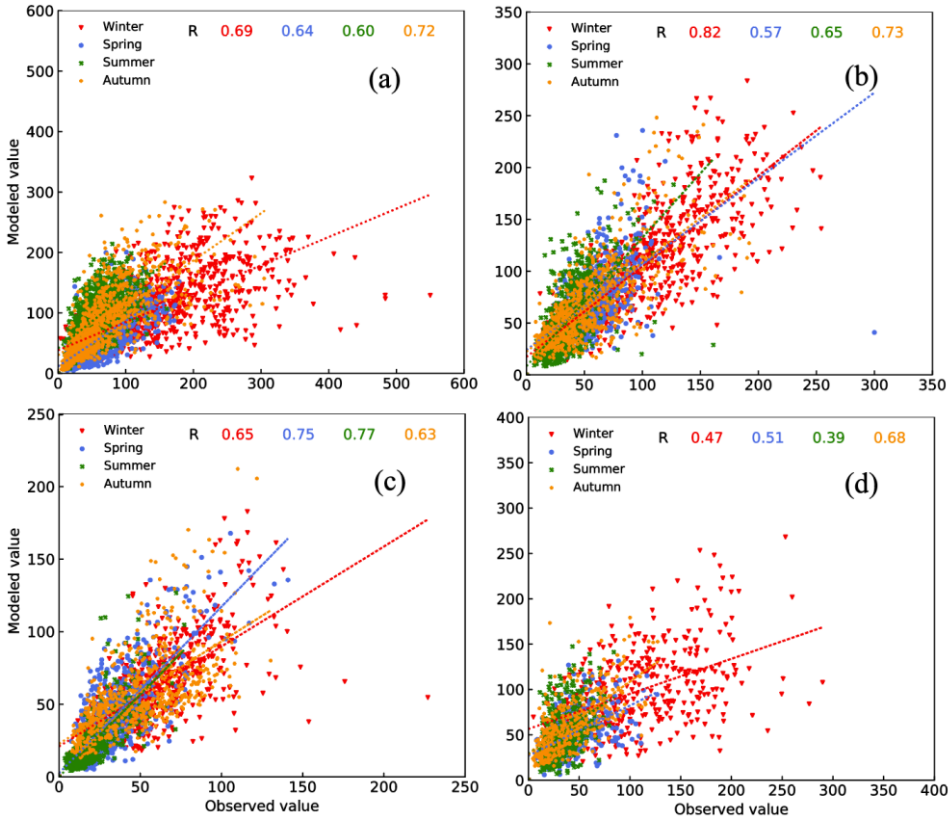
Winter
Spring
Summer
Autumn
R
0.69
0.64
0.60
0.72
(a)
Modeled value
0.82
0.57
0.65
0.73
(b)
0.65
0.75
0.77
0.63
(c)
Observed value
0.47
0.51
0.39
0.68
(d)

760

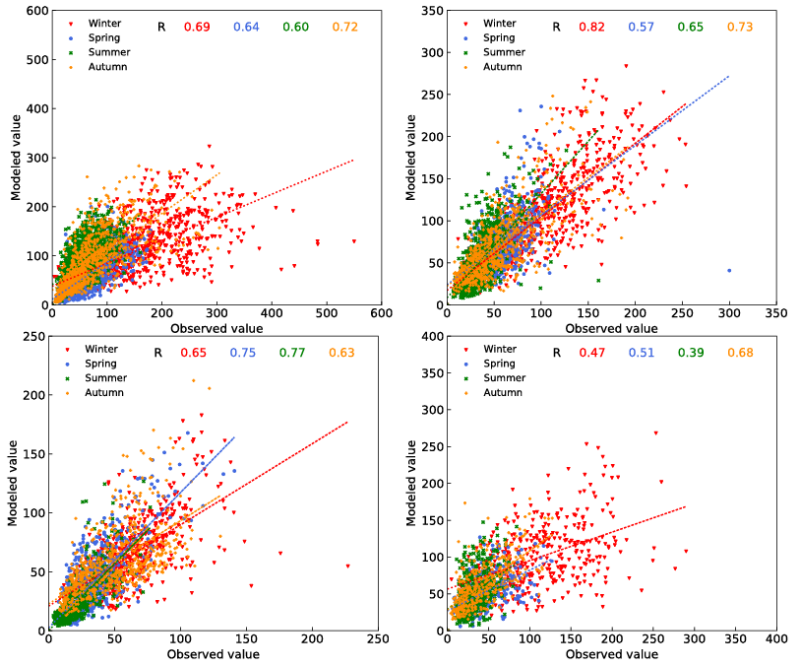

Figure 3. Scatter plots and correlation coefficients of daily $PM_{2.5}$ concentrations (~~μ~~g m^{-3}) between observed and simulated values in different seasons in the (a) NCP, (b) YRD, (c) PRD, and (d) SCB regions.

Formatted: Superscript

765

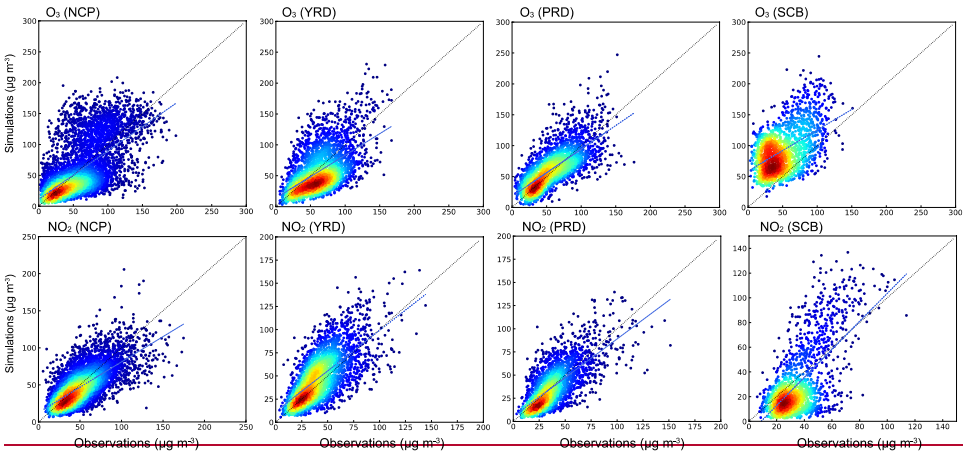

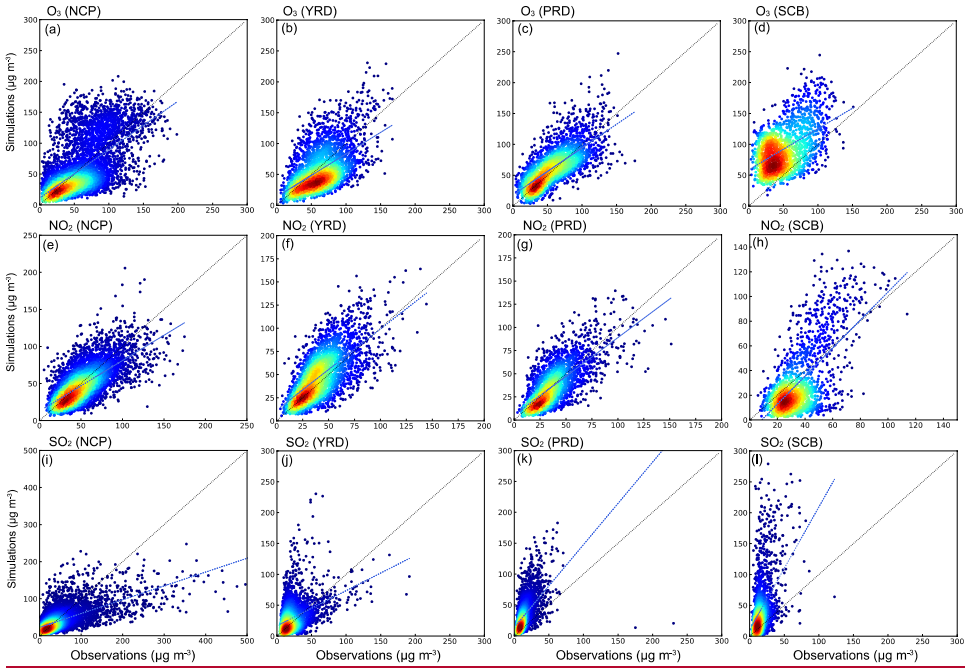

Figure 4. Scatter plots of modelled and observed hourly concentrations of (a-d) O_3, (e-h) ~~and~~ NO_2 and (i-l) SO_2 in the NCP, YRD, PRD, and SCB regions.

Formatted: Subscript

770

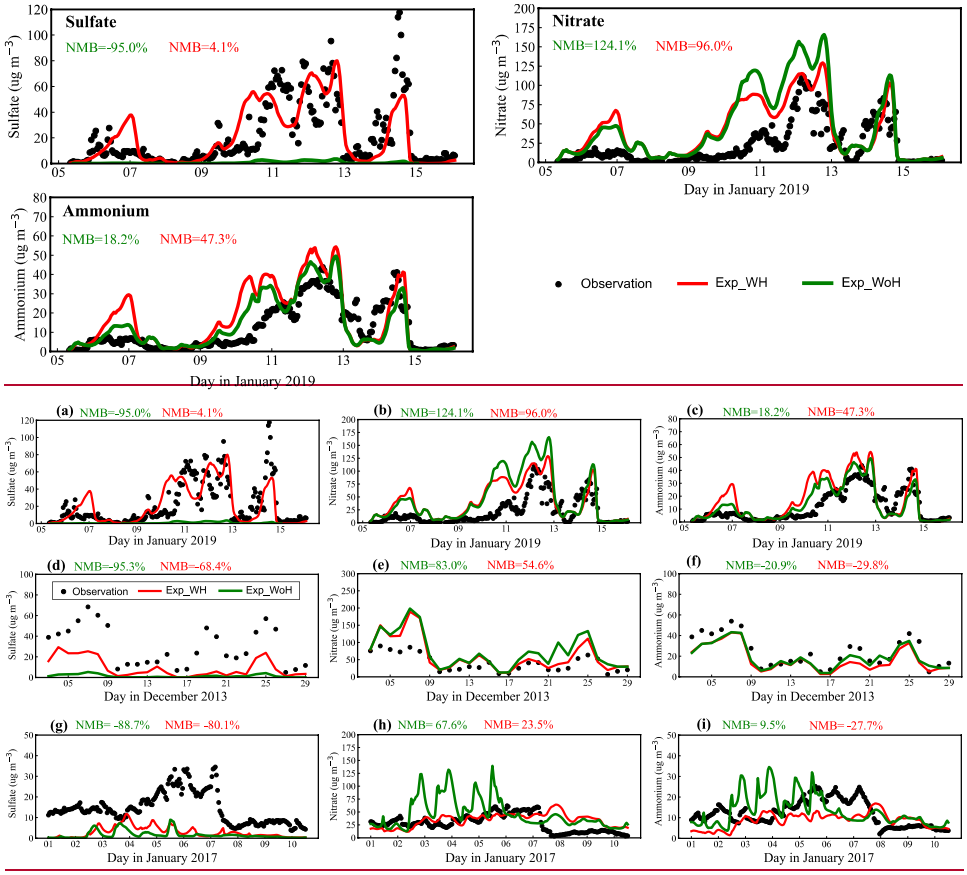

Figure 5. Observed and simulated hourly SIA concentrations from the Exp_WH and Exp_WoH experiments at the (a-c) Langfang, (d-f) Nanjing and (g-i) Chengdu sites.

775

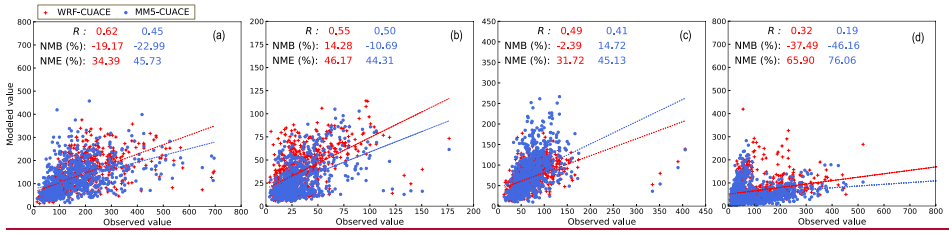

Figure 6. Scatter plots of simulated, with (blue) MM5/CUACE and (red) WRF/CUACE, and observed daily concentrations of (a) $PM_{2.5}$, (b) O_3, (c) NO_2 and (d) SO_2.

Formatted: Subscript

Formatted: Subscript

Formatted: Subscript

Formatted: Subscript

Table 1 Uptake coefficients for reactions (14)-(22).

Gas species	Uptake coefficients	References
H_2O_2	$\gamma = 1.0 \times 10^{-4}$	Bian and Zender (2003)
HNO_3	$\gamma = 1.0 \times 10^{-1}$	Seisel et al. (2004)
HO_2	$\gamma = 1.0 \times 10^{-1}$	Phadnis and Carmichael (2000)
N_2O_5	γ	Wang et al. (2012)
NO_2	$= \begin{cases} \gamma_{low}, RH \in [0,50\%] \\ \gamma_{low} + \frac{(\gamma_{high} - \gamma_{low})}{(RH_{max} - 0.5)} * (RH - 0.5), RH \in (50\%, RH_{max}] (\gamma_{high} -) \\ \times (RH - 0.5), RH \in (50\%, RH_{max} \\ \gamma_{high}, RH \in (RH_{max}, 100\%] \end{cases}$	Zheng et al. (2015)
NO_3		
SO_2		
O_3	$\gamma = 3.0 \times 10^{-5}$	Michel et al. (2003)
OH	$\gamma = 1.0 \times 10^{-4}$	Zhang and Carmichael (1999)
~~SO_2~~	~~$\gamma = \begin{cases} \gamma_{low}, RH \in [0,50\%] \\ \gamma_{low} + (\gamma_{high} - \gamma_{low})/(RH_{max} \\ \times (RH - 0.5), RH \in (50\%, RH_{max} \\ \gamma_{high}, RH \in (RH_{max} \end{cases}$~~	~~Zheng et al. (2015)~~

* The γ_{low} and γ_{high} are the lower and upper limits of γ values. The RH_{max} is the RH value at which the γ reaches the upper limit. The values of γ_{low}, γ_{high} and RH_{max} are referred to the work of Zheng et al. (2015) and Wang et al., (2012). That is, values of γ_{low} for N_2O_5, NO_2, NO_3 and SO_2 are 1E-3, 4.4E-5, 0.1 and 2E-5, respectively corresponding to the values of γ_{high} at 0.1, 2E-4, 0.23, 5E-5. The RH_{max} is 70 % for N_xO_y, and is 100 % for SO_2.

Table 2 Physical parameterization schemes used in the modelling study.

Physical management	Parameterization	References
Microphysics scheme	Lin	Lin et al. (1983)
Shortwave radiation	Goddard	Chou and Suarez (1994)
Longwage radiation	RRTM	Mlawer et al. (1997)
Land surface scheme	Noah	Chen and Dudhia (2001)
Boundary layer scheme	MYJ	Janjić (1994)
Cumulus scheme	Grell-3D	Grell (1993)

Formatted Table

Formatted: Font: 8 pt (×31)

Formatted: Subscript

Formatted Table

Formatted: Font: 8 pt

Formatted: Line spacing: 1.5 lines, Don't snap to grid

Formatted: Font: 五号, Not Bold

Formatted: Font: 五号, Not Bold

Formatted: Font: 五号, Not Bold

Formatted: Font: (Default) Times New Roman

790 **Table 3 Statistical metrics for hourly $PM_{2.5}$ in four haze contaminated areas (2013–2017), in which bold, normal , and italic font for MFB and MFE correspond to the "excellent", "good", and "average" levels in Morris et al. (2005), respectively.**

	R	MB μg m^{-3}	ME μg m^{-3}	NMB %	NME %	MFB %	MFE %
NCP	0.59	-5.0	44.5	-5.4	47.5	3.3	49.1
Winter	0.59	-45.0	67.7	-28.4	42.7	-22.5	47.0
Spring	0.57	-9.5	28.0	-14.0	41.1	-20.7	47.4
Summer	0.47	33.9	42.9	55.1	69.8	*44.9*	*56.3*
Autumn	0.63	-0.8	39.2	-0.9	45.4	9.0	45.9
YRD	0.71	12.9	26.9	21.8	45.3	21.1	42.9
Winter	0.75	6.0	30.6	6.4	32.5	**8.5**	**34.1**
Spring	0.49	14.2	26.3	25.4	47.1	19.1	40.0
Summer	0.56	16.4	23.3	47.8	67.9	26.7	49.4
Autumn	0.66	15.1	27.3	28.7	51.8	29.5	48.0
PRD	0.68	5.3	17.1	13.1	42.1	8.6	40.1
Winter	0.56	3.0	20.5	5.0	34.6	**5.5**	**34.4**
Spring	0.64	6.9	17.6	19.5	49.7	4.2	45.6
Summer	0.68	2.8	8.5	14.8	44.4	5.9	39.0
Autumn	0.54	8.6	21.8	17.7	45.2	18.3	41.9
SCB	0.59	7.6	31.3	12.2	50.3	*20.7*	*51.4*
Winter	0.41	-13.3	46.7	-11.5	40.4	-8.3	45.2
Spring	0.49	4.1	22.4	8.4	45.9	11.4	46.1
Summer	0.40	21.6	28.2	60.4	78.6	*38.7*	*58.9*
Autumn	0.58	15.9	28.2	31.4	55.7	*37.2*	*54.3*

795 **Table 4 Statistical metrics for O_3 and NO_2 concentrations. Criteria for O_3 are from the EPA (2005, 2007). The values that do not meet the criteria are in bold.**

Variables		NCP	YRD	PRD	SCB	Criteria
O_3	R	0.64	0.66	0.77	0.60	
	NMB (%)	-0.60	-8.21	7.24	**77.61**	⩽±15
	IOA	0.80	0.80	0.87	0.67	
NO_2	R	0.60	0.64	0.67	0.57	
	NMB (%)	-6.62	14.42	-2.45	-14.36	
	IOA	0.77	0.77	0.81	0.71	
SO_2	R	0.65	0.41	0.57	0.47	
	NMB (%)	-15.48	24.55	125.74	159.44	
	IOA	0.72	0.60	0.49	0.32	